



# Phylogeography and Diversity Among Populations of the Toxigenic Benthic Dinoflagellate *Prorocentrum* From Coastal Reef Systems in Mexico

## OPEN ACCESS

### Edited by:

Elisabete Valério,  
Instituto Nacional de Saúde Doutor  
Ricardo Jorge (INSA), Portugal

### Reviewed by:

Haifeng Gu,  
Third Institute of Oceanography, State  
Oceanic Administration, China  
Albert Reñé,  
Instituto de Ciencias del Mar, Consejo  
Superior de Investigaciones  
Científicas (CSIC), Spain

### \*Correspondence:

Lorena M. Durán-Riveroll  
lduran@conacyt.mx  
Allan D. Cembella  
allan.cembella@awi.de

### †ORCID:

Allan D. Cembella  
orcid.org/0000-0002-1297-2240  
Lorena M. Durán-Riveroll  
orcid.org/0000-0001-8805-7228  
Yuri B. Okolodkov  
orcid.org/0000-0003-3421-3429  
Cora Hörstmann  
orcid.org/0000-0002-0097-2454  
Uwe John  
orcid.org/0000-0002-1297-4086

### Specialty section:

This article was submitted to  
Global Change and the Future Ocean,  
a section of the journal  
Frontiers in Marine Science

Received: 29 May 2021

Accepted: 14 September 2021

Published: 15 October 2021

### Citation:

Cembella AD, Durán-Riveroll LM,  
Tarazona-Janampa UI, Okolodkov YB,  
García-Sandoval R, Krock B,  
Hörstmann C and John U (2021)  
Phylogeography and Diversity Among  
Populations of the Toxigenic Benthic  
Dinoflagellate *Prorocentrum* From  
Coastal Reef Systems in Mexico.  
Front. Mar. Sci. 8:716669.  
doi: 10.3389/fmars.2021.716669

Allan D. Cembella<sup>1\*†</sup>, Lorena M. Durán-Riveroll<sup>1,2\*†</sup>, Ulrike I. Tarazona-Janampa<sup>1,3,4</sup>,  
Yuri B. Okolodkov<sup>5†</sup>, Ricardo García-Sandoval<sup>6</sup>, Bernd Krock<sup>1</sup>, Cora Hörstmann<sup>1†</sup> and  
Uwe John<sup>1,7†</sup>

<sup>1</sup> Alfred-Wegener-Institut, Helmholtz-Zentrum für Polar- und Meeresforschung, Bremerhaven, Germany,

<sup>2</sup> CONACYT-Departamento de Biotecnología Marina, Centro de Investigación Científica y de Educación Superior de Ensenada, Ensenada, Mexico, <sup>3</sup> International Max Planck Research School, Max Planck Institute for Marine Microbiology, Bremen, Germany, <sup>4</sup> Laboratorio de Microbiología Molecular y Genómica Bacteriana, Universidad Científica del Sur, Lima, Peru, <sup>5</sup> Instituto de Ciencias Marinas y Pesquerías, Universidad Veracruzana, Boca del Río, Mexico, <sup>6</sup> Departamento de Biología Comparada, Facultad de Ciencias, Universidad Nacional Autónoma de México, Coyoacán, Mexico, <sup>7</sup> Helmholtz Institute for Functional Marine Biodiversity, Oldenburg, Germany

The marine dinoflagellate genus *Prorocentrum* Ehrenberg comprises many species occupying primarily benthic or epiphytic habitats, particularly in tropical and sub-tropical waters. Despite concerted efforts to establish phylogenetic associations, there remain unresolved issues in defining morphospecies and membership in species complexes. The study described herein addressed the inter- and infraspecific relationships of members of the *Prorocentrum lima* and *Prorocentrum hoffmannianum* species complexes (PLSC and PHSC, respectively) by applying multivariate approaches in morphotaxonomy, molecular phylogenetics and chemodiversity to establish affinities among multiple clonal isolates. Morphotaxonomic analysis showed consistency with classical morphospecies descriptors, and high variability in cell size and dimensions, but did not challenge current species complex concepts. Phylogenetic analysis of ITS/5.8S rDNA sequences from isolates from the Gulf of California, Caribbean Sea, and Gulf of Mexico coasts compared with archived global GenBank sequences served to define five consistent clades with separation of the PLSC and PHSC. Secondary structure modeling of ITS2 rRNA variation based on compensatory base changes (CBC) was effective in resolving details of the respective species complexes and even indicated putative incipient or cryptic speciation due to potential hybridization barriers. This study represents the largest ( $n = 67$  isolates) chemodiversity analysis of polyketide-derived toxins associated with diarrhetic shellfish poisoning (DSP) from a benthic dinoflagellate genus. Relative composition of some analogs (OA, OA-D8, DTX1, DTX1a, and DTX1a-D8), including two new undescribed isomers, distinguished *P. lima* from *P. hoffmannianum sensu lato*, but without clear associations with substrate type or geographical origin. Although all *P. lima* and most (one exception) *P. hoffmannianum* were toxigenic, the total cell toxin content could not be linked at the species level.

This research demonstrates that clonal chemodiversity in toxin composition cannot yet be effectively applied to define ecological niches or species interactions within local assemblages. Phylogenetic analysis of the ITS/5.8 rDNA, particularly when combined with secondary structure modeling, rather than only a comparison of LSU rDNA sequences, is a more powerful approach to identify cryptic speciation and to resolve species complexes within benthic dinoflagellate groups.

**Keywords:** *Prorocentrum lima*, species complex, epibenthic dinoflagellates, diarrhetic shellfish poisoning, polyether toxins, rDNA variation, chemodiversity

## INTRODUCTION

Benthic species of the dinoflagellate genus *Prorocentrum* Ehrenb. (Prorocentrales: Prorocentraceae) are globally distributed from polar latitudes to the tropics, but comprise a higher percentage of the epibenthic microflora in tropical and subtropical coastal waters (Durán-Riveroll et al., 2019). Although not all *Prorocentrum* species are toxigenic, the production of polyether toxins is a common trait among benthic species, such as *Prorocentrum concavum* Y. Fukuyo, *Prorocentrum faustiae* S. L. Morton, *Prorocentrum hoffmannianum* (syn. *Prorocentrum belizeanum* M. A. Faust), *Prorocentrum lima* (syn. *Prorocentrum arenarium* M. A. Faust), and *Prorocentrum maculosum* M. A. Faust, but these toxins are essentially absent or have not been confirmed from planktonic taxa. The polyether toxins found among *Prorocentrum* species include okadaic acid (OA) and at least two dozen dinophysistoxin (DTX) analogs, plus related polyketides of uncertain toxicity (Hu et al., 2010). The toxins from these benthic species can accumulate in suspension-feeding shellfish and thereby cause a complex syndrome known as diarrhetic shellfish poisoning (DSP) in human consumers of contaminated shellfish.

*Prorocentrum lima* (Ehrenb.) F. Stein 1878 emend. Nagahama et al. (2011) is one of the most widely distributed species of the genus. In tropical and sub-tropical coastal ecosystems (Durán-Riveroll et al., 2019) the species is commonly found as an epiphyte upon macroalgae, seagrasses, and inanimate substrates (Tarazona-Janampa et al., 2020). There is limited and somewhat contradictory evidence of biotic substrate preferences for benthic *Prorocentrum* (Boisnoir et al., 2019), but little is known about the basis of the selective mechanisms, chemical ecological interactions or potential effect on toxin production or composition. Recent molecular genetic studies of *P. lima* have revealed a high genetic variability, apart from (and not always consistent with) great variability in some morphological features (cell shape, length and width, number and shape of marginal pores). Accordingly, these similar but unresolved taxa were assigned to the “*P. lima* complex” as proposed by Aligizaki (2009), and in subsequent literature [e.g., Moreira-González et al. (2019)]. Herein these taxa are referred to as members of the *P. lima* species complex (PLSC).

*Prorocentrum* species from coastal and reef systems of Mexico commonly include *P. hoffmannianum* M. A. Faust 1990, often coinciding with *P. lima* (Durán-Riveroll et al., 2019). As in the current study, specimens of *P. lima*

and *P. hoffmannianum sensu stricto* are well distinguished morphologically within field populations and usually in clonal culture. Nevertheless, unresolved issues regarding the synonymy and affinities with other described morphospecies closely related to *P. hoffmannianum* remain under debate. Combined molecular genetic and morphological analysis for *P. hoffmannianum* and relatives such as *P. belizeanum* (Herrera-Sepúlveda et al., 2015) have demonstrated the existence of a *P. hoffmannianum* species complex (PHSC), but not resolved the association with the PLSC. The challenge addressed in the current study at the infraspecific level was to determine affinities within and between the PLSC and PHSC by multivariate application of morphological, molecular phylogenetic, and toxin chemodiversity techniques.

*Prorocentrum rhathymum* A. R. Loeblich et al. (1979) is morphologically distinct from both the PLSC and PHSC, but remains an enigma with uncertain species distinction, e.g., from *Prorocentrum mexicanum* B. F. Osorio (Steidinger and Tangen, 1996; Faust and Gulledege, 2002; Cortés-Altamirano and Sierra-Beltrán, 2003), based on both morphological and ecological (habitat) differences. Molecular phylogenetic analysis of *P. rhathymum* strains from Florida (An et al., 2010) vs. *P. cf. rhathymum* from Korea has served to highlight inconsistencies in species level discrimination (Lim et al., 2013). The most recent molecular phylogenetic analysis of *Prorocentrum* from the eastern Caribbean Sea based on LSU rDNA sequences clusters *P. mexicanum* closely together *P. rhathymum* but basal to and distinct from the paraphyletic PLSC clade (Chomérat et al., 2019).

Benthic dinoflagellate species are quite well described morphologically from Latin America (reviewed in Durán-Riveroll et al. (2019) but there are many gaps in known phylogeographical distribution, few confirmed records of cell toxicity or toxin composition and a paucity of molecular confirmation of species identities and phylogenetic relationships. This poor state of knowledge also applies to benthic *Prorocentrum* species although members of the genus have been reported and described from both the Pacific [for references, see Okolodkov and Gárate-Lizárraga (2006); Gárate-Lizárraga et al. (2007)], and Gulf of Mexico and Caribbean coasts of Mexico (Okolodkov et al., 2007, 2014; Barón-Campis et al., 2014; Almazán-Becerril et al., 2015; Aguilar-Trujillo et al., 2017).

The work presented herein comprises a comparative analysis of cell morphotaxonomy, toxigenicity and molecular diversity of clonal isolates from populations of benthic *Prorocentrum* from three coastal marine ecosystems, representing the Gulf of

California, Gulf of Mexico, and Caribbean Sea. The aim was to identify diversity patterns within and among geographical populations and substrate affinities and to define coherences and discrepancies (e.g., putative cryptic species) based on these different characteristics.

## MATERIALS AND METHODS

### Isolation and Culture of *Prorocentrum*

Samples for benthic dinoflagellate isolation were collected from targeted locations along the Gulf of California, Gulf of Mexico, and Caribbean coasts of Mexico (**Figure 1**). Primary collection sites were within Bahía de La Paz (Baja California Sur (24°09′30.01″N 110°19′12.10″W), the Veracruz Reef System (VRS), Veracruz (19°11′54.10″N, 96° 4′0.70″W), and Puerto Morelos, Quintana Roo (20°50′48.55″N, 86°52′30.53″W) (**Table 1**). Epibenthic substrates were collected from seagrass beds (*Thalassia testudinum* Banks ex König) and from polypropylene ropes indicating swimming areas by snorkeling in shallow water along sandy shores. Specimens were also collected along rocky shores, from attached and floating macroalgae, *Ulva* (Chlorophyta: Ulvaceae), *Laurencia* (Rhodophyta: Rhodomelaceae), *Sargassum* and *Padina* spp. (Phaeophyceae: Sargassaceae and Dictyotaceae, respectively), and detritus on sediments and buoys.

Live samples were transported with site water in 50 mL conical plastic centrifuge tubes in an ice chest with ice packs to maintain ambient temperature around 24°C during the transport to the laboratory at Instituto de Ciencias del Mar y Limnología, Universidad Nacional Autónoma de México (ICMyL-UNAM), Mexico City. Substrate specimens and surrounding seawater were examined for epibenthic dinoflagellates in Petri plates under a stereo-dissecting microscope (Discovery.V8, Zeiss, Göttingen, Germany). Substrates were gently brushed and single-cells of epibenthic dinoflagellates were isolated by micropipette into sterile 96-well microplates containing 300 µL 50%-strength GSe growth medium (Blackburn et al., 2001) modified without soil extract and prepared from autoclaved seawater filtered through sand, activated carbon and 1 µm-cartridge-filters. The growth medium, supplemented with GeO<sub>2</sub> (final concentration: 2.5 mg L<sup>-1</sup>) to inhibit diatom growth, was prepared from heat-sterilized seawater stock at salinity 36. Clonal isolates were cultured by incubation at 25 ± 1°C on a 12:12 h light:dark cycle and illumination of 50 µmol photons m<sup>-2</sup> s<sup>-1</sup>.

Once dinoflagellate cell division was observed (around 6–8 cells per well) after 10–12 days, preliminary cultures were transferred into 24-well microplates, each well containing 2 mL growth medium, and after subsequent growth, into 60 × 15 mm sterile plastic Petri plates with 15 mL 50%-strength GSe seawater medium. Clonal isolates were maintained at ICMYL-UNAM, Mexico under the same conditions for morphological species identification by microscopy.

Subcultures of the collection of *Prorocentrum* isolates ( $n = 69$ ) were transferred to the culture facilities at the Alfred Wegener Institute (AWI), Bremerhaven, Germany, for production of cells for rDNA and toxin analysis. These stock cultures were initially

grown in plastic Petri plates on 50%-strength GSe, and then acclimated to K medium (Keller et al., 1987) added as enrichment to 0.2 µm-filtered and autoclaved North Sea seawater at salinity 33. All reference and experimental cultures were maintained at 24 ± 1°C on a light:dark cycle of 14:10 h and illumination of 86 µmol photons m<sup>-2</sup> s<sup>-1</sup>.

Exponentially growing *Prorocentrum* cells were harvested from Petri plates for rDNA analysis, and after cell enumeration by microscopy (target *ca.* 10<sup>6</sup> cells), were collected by centrifugation at 3,220 × *g* for 15 min at 4°C (Eppendorf 5810R, Hamburg, Germany). After removal of the aqueous supernatant, the pellet was transferred to a 2 mL microcentrifuge tube for total DNA extraction from fresh pellets.

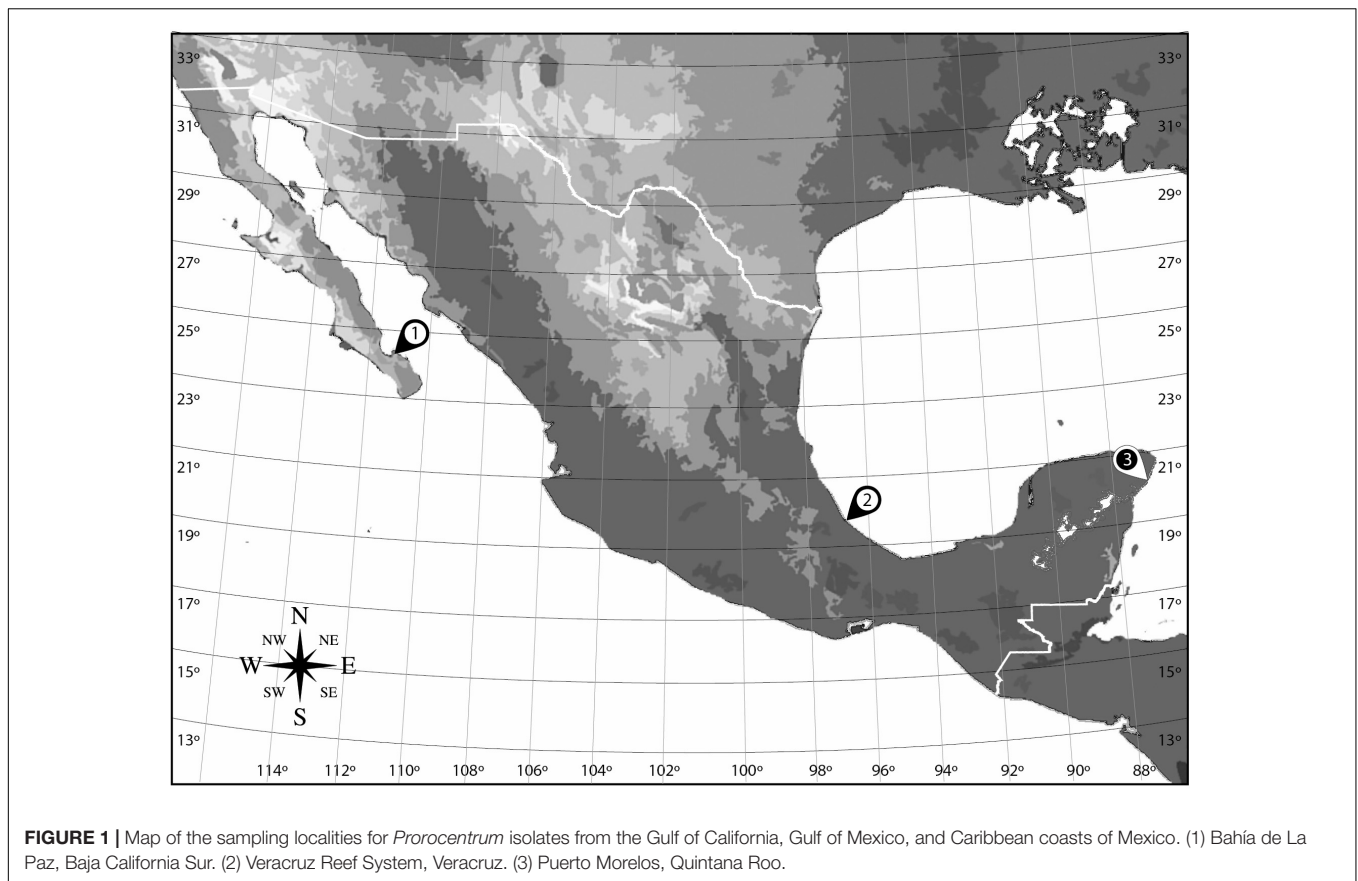
Harvest details of actively growing *Prorocentrum* cultures and cell enumeration for DSP toxin analysis followed previously described methods (Tarazona-Janampa et al., 2020). In brief, cultured cells were harvested from plastic Petri plates by multiple centrifugation steps. The final cell pellets in 2 mL FastPrep tubes were placed in a thermomixer (Eppendorf, Hamburg Germany) at 100°C for 5 min to inactivate esterase enzymes that could modify the toxin profile. Cell pellets were stored frozen (–20°C) for later extraction.

### Morphological Description of *Prorocentrum* Isolates

Specimens of *Prorocentrum* isolates from early phase stable cultures were examined for morphological characteristics by both light and scanning electron microscopy (SEM). Teratological forms rather common in cultures were avoided. Provisional assignment to morphospecies was conducted by light microscopy (Motic BA310E, Hong Kong, SAR China) at 1000× magnification and from micrographs taken with a digital camera (6 MP, Moticam S6, Motic, Hong Kong, SAR China). Further details of the thecal plates were studied after staining cells with 0.2% Calcofluor White M2R in aqueous solution (Fritz and Triemer, 1985). Cells were observed under epifluorescence microscopy (Axio Scope.A1, Carl Zeiss, Oberkochen, Germany) with filter set 18 shift free EX BP 390–420 (excitation), BS FT 425 (optical divider), and EM LP 450 (emission), using the Plan-Neofluar 40×/0.75 and 63×/0.95 Korr objectives (total magnification 400× and 630×, respectively). Photomicrographs were taken with a Carl Zeiss Axiocam 506 color camera (6 MP) using the ZEN 2012 SP2 program (Carl Zeiss Microscopy GmbH, Göttingen, Germany).

Cell dimensions ( $n = 30$ ) for morphometric analysis were determined from cells either live or freshly fixed in Lugol's iodine or neutralized 4% formaldehyde and examined with a light microscope (Motic BA310E, Hong Kong, SAR China) at 400× magnification. Cell size was estimated from digital camera (6 MP, Moticam S6, Motic, Hong Kong, SAR China) images captured with Motic Images Advanced 3.0 software, previously calibrated with a micrometer.

Cultured dinoflagellate cells for SEM were fixed with 2% glutaraldehyde for 90 min. Specimens were washed in 1.5 mL distilled water (5°C) and centrifuged at 1,200 × *g* at 5°C for 6 min. The wash procedure was repeated four times. Samples



(1.5 mL each) underwent a graded ethanol dehydration series (10, 30, 50, 70, 90, and 99%), with centrifugation as for the sample wash at each dehydration step. Finally, 250  $\mu$ L of hexamethyldisilazane air-drying agent was placed upon the sample on aluminum SEM stubs, and specimens were gold sputter-coated for 5 min. Dinoflagellate cells were observed with a JEOL JSM6360LV SEM equipped with a backscattered electron detector under 8 kV voltage acceleration and at 15 mm working distance.

## DNA Sequencing and Molecular Phylogenetic Analysis

### DNA Extraction and Sequencing

Total DNA was extracted and processed with the Genomic DNA PowerSoil kit (Macherey-Nagel, Düren, Germany), following the manufacturer's protocol. The cell pellet for each isolate was extracted in a 2 mL microcentrifuge tube with 400  $\mu$ L SL1 lysis buffer (Macherey-Nagel, Düren, Germany) by homogenization in a FastPrep FP120 (Bio 101, Thermo Savant, Illkirch, France) at 6.5  $m s^{-1}$  for 45 s. The DNA purity and quantity were assessed by UV-spectroscopy with a NanoDrop ND-1000 system (Peqlab, Erlangen, Germany) and DNA integrity was confirmed by 1% agarose gel electrophoresis.

The D1/D2 region of the 28S large subunit (LSU) rDNA and the internal transcribed spacer (ITS) region (including the ITS1, 5.8S subunit, and ITS2 sequences; referred to hereafter

as ITS/5.8S) were amplified from each total DNA extract by polymerase chain reaction (PCR). The forward and reverse primers for LSU amplification were: D1R-F (5'-ACC CGC TGA ATT TAA GCA TA-3') and D2C-R (5'-CCT TGG TCC GTG TTT CAA GA-3'), respectively. The forward and reverse primers for ITS/5.8 amplification were: ITS a (5'-CCA AGC TTC TAG ATC GTA ACA AGG (ACT)TC CGT AGG T-3') and ITS b (5'-CCT GCA GTC GAC A(GT)A TGC TTA A(AG)T TCA GC(AG) GG-3'), respectively. Reaction conditions were as follows: HotMaster Taq<sup>®</sup> (5 Prime, Hamburg, Germany) buffer 1 $\times$ , 0.1 mM of dNTPs, 0.1 mM of each forward and reverse primer and 1.25 units of Taq polymerase were added to 10–30 ng of the extracted genomic DNA in total reaction volumes of 50  $\mu$ L. For the 28S rDNA amplifications, the reactions were subjected to the following thermocycling conditions: one cycle at 95°C for 7 min; 35 cycles at 94°C for 45 s, hold at 54°C for 2 min, 70°C for 1.5 min; and a final extension at 70°C for 5 min. The thermocycling conditions for the ITS/5.8 amplifications were: one cycle at 94°C for 4 min; 9 cycles at 94°C for 50 s, hold at 60°C for 40 s and then at 70°C for 1 min; 29 cycles 94°C for 45 s, then at 50°C for 45 s, 70°C for 1 min; and a final 5 min extension step at 70°C.

Samples were kept at 4°C until analysis on 1% agarose gel to ensure the expected amplification products were present. After PCR amplification LSU amplicons were sequenced and ITS/5.8S amplicons were subsequently cloned into the vector provided with the TOPO TA Cloning<sup>®</sup> kit (Invitrogen, Carlsbad,

**TABLE 1** | Cultured clonal isolates ( $n = 69$ ) of *Prorocentrum* species from locations on the Gulf of California, Gulf of Mexico, and Caribbean coasts, indicating locality of origin and substrate type, and provisional species assignment according to morphological characteristics.

Isolate number	Locality of origin	Substrate type	Cell dimensions (mean $\pm$ SD)			Provisional morphospecies	
			L ( $\mu\text{m}$ )	W ( $\mu\text{m}$ )	L/W ratio		
PA44	BLP	Sediment w/detritus (Ochrophyta)	35.31 $\pm$ 1.89	26.29 $\pm$ 1.46	1.34 $\pm$ 0.06	<i>P. lima</i>	
PA46			34.07 $\pm$ 2.89	24.50 $\pm$ 1.53	1.39 $\pm$ 0.07		
PA47		<i>Ulva</i> sp. (Chlorophyta)	35.73 $\pm$ 2.20	28.05 $\pm$ 2.29	1.28 $\pm$ 0.12		
PA48			35.26 $\pm$ 2.55	24.89 $\pm$ 1.65	1.42 $\pm$ 0.07		
PA49			36.91 $\pm$ 2.03	27.55 $\pm$ 1.07	1.34 $\pm$ 0.07		
PA50			35.73 $\pm$ 1.86	23.68 $\pm$ 1.57	1.52 $\pm$ 0.13		
PA51		Sediment w/detritus (Ochrophyta)	37.13 $\pm$ 1.26	28.29 $\pm$ 1.93	1.32 $\pm$ 0.08		
PA53		<i>Sargassum</i> sp. (Ochrophyta)	35.62 $\pm$ 1.11	25.61 $\pm$ 1.18	1.39 $\pm$ 0.06		
PA69		AAR	Unidentified green algae (Chlorophyta)	37.19 $\pm$ 1.54	26.97 $\pm$ 1.11		1.38 $\pm$ 0.03
PA76			37.45 $\pm$ 2.10	28.61 $\pm$ 1.81	1.31 $\pm$ 0.06		
PA77			37.53 $\pm$ 2.21	27.41 $\pm$ 1.63	1.37 $\pm$ 0.05		
PA1	IV	<i>Thalassia testudinum</i> (Tracheophyta)	34.14 $\pm$ 2.08	25.83 $\pm$ 1.72	1.32 $\pm$ 0.07		
PA2			35.49 $\pm$ 1.87	25.39 $\pm$ 1.40	1.40 $\pm$ 0.05		
PA3			38.11 $\pm$ 2.34	27.51 $\pm$ 1.99	1.39 $\pm$ 0.09		
PA5			35.63 $\pm$ 1.53	25.90 $\pm$ 1.08	1.38 $\pm$ 0.07		
PA6			40.43 $\pm$ 1.54	27.95 $\pm$ 1.42	1.45 $\pm$ 0.10		
PA7			34.73 $\pm$ 1.84	24.67 $\pm$ 1.11	1.41 $\pm$ 0.10		
PA8			38.34 $\pm$ 2.38	27–46 $\pm$ 1.78	1.40 $\pm$ 0.11		
PA9		<i>Laurencia</i> sp. (Rhodophyta)	38.95 $\pm$ 1.80	30.06 $\pm$ 1.13	1.30 $\pm$ 0.06		
PA11		<i>Thalassia testudinum</i> (Tracheophyta)	34.35 $\pm$ 1.42	24.64 $\pm$ 2.21	1.40 $\pm$ 0.12		
PA12			32.47 $\pm$ 1.81	24.79 $\pm$ 1.22	1.31 $\pm$ 0.06		
PA13			33.12 $\pm$ 1.95	24.63 $\pm$ 1.27	1.35 $\pm$ 0.09		
PA17		<i>Laurencia</i> sp. (Rhodophyta)	40.96 $\pm$ 3.02	27.95 $\pm$ 2.97	1.48 $\pm$ 0.15		
PA18			33.56 $\pm$ 2.39	25.21 $\pm$ 1.62	1.34 $\pm$ 0.09		
P019			39.71 $\pm$ 1.70	28.98 $\pm$ 1.42	1.37 $\pm$ 0.07		
PA25		<i>Thalassia testudinum</i> (Tracheophyta)	36.76 $\pm$ 1.46	25.43 $\pm$ 1.09	1.45 $\pm$ 0.05		
PA61		PLV	<i>Padina</i> sp. (Ochrophyta)	38.66 $\pm$ 1.51	29.01 $\pm$ 1.13		1.33 $\pm$ 0.05
PA62				38.20 $\pm$ 0.82	27.45 $\pm$ 1.29		1.39 $\pm$ 0.06
PA63				36.74 $\pm$ 2.36	27.25 $\pm$ 1.85		1.35 $\pm$ 0.09
PA64				33.90 $\pm$ 1.70	27.47 $\pm$ 1.73		1.24 $\pm$ 0.09
PA65			38.65 $\pm$ 2.47	28.42 $\pm$ 1.58	1.37 $\pm$ 0.08		
PA66			37.89 $\pm$ 1.36	26.45 $\pm$ 1.19	1.43 $\pm$ 0.06		
PA67			36.08 $\pm$ 2.34	27.16 $\pm$ 1.89	1.33 $\pm$ 0.06		
PA68			36.36 $\pm$ 2.08	26.93 $\pm$ 1.94	1.35 $\pm$ 0.07		
PA70			46.48 $\pm$ 2.18	38.61 $\pm$ 2.90	1.21 $\pm$ 0.08	<i>P. hoffmannianum</i>	
PA71			40.21 $\pm$ 1.59	34.13 $\pm$ 2.24	1.18 $\pm$ 0.08		
PA72			37.34 $\pm$ 1.81	26.09 $\pm$ 1.67	1.44 $\pm$ 0.09	<i>P. lima</i>	
PA73			47.41 $\pm$ 2.18	39.33 $\pm$ 1.87	1.21 $\pm$ 0.05	<i>P. hoffmannianum</i>	
PA74			43.20 $\pm$ 1.98	34.13 $\pm$ 2.24	1.27 $\pm$ 0.10		
PA75		37.74 $\pm$ 1.86	28.87 $\pm$ 1.86	1.31 $\pm$ 0.07	<i>P. lima</i>		
PA78	Unidentified brown algae (Ochrophyta)		46.36 $\pm$ 1.33	38.36 $\pm$ 1.36	1.21 $\pm$ 0.04		
PA79			35.41 $\pm$ 1.82	26.67 $\pm$ 1.46	1.33 $\pm$ 0.07		
PA80			40.76 $\pm$ 2.08	28.45 $\pm$ 1.47	1.43 $\pm$ 0.07		
PA81			36.05 $\pm$ 1.83	26.92 $\pm$ 1.48	1.34 $\pm$ 0.09		
PA82			36.14 $\pm$ 1.73	27.60 $\pm$ 1.33	1.31 $\pm$ 0.07		
PA83			37.57 $\pm$ 1.37	27.69 $\pm$ 1.13	1.36 $\pm$ 0.06		
PA84			34.76 $\pm$ 1.29	23.22 $\pm$ 1.21	1.33 $\pm$ 0.06		
PA85			44.76 $\pm$ 2.10	37.06 $\pm$ 1.58	1.21 $\pm$ 0.05	<i>P. hoffmannianum</i>	
PA86			36.55 $\pm$ 1.62	26.80 $\pm$ 1.09	1.37 $\pm$ 0.07	<i>P. lima</i>	
PA87			36.70 $\pm$ 1.54	27.97 $\pm$ 1.19	1.31 $\pm$ 0.07		
PA88			34.95 $\pm$ 2.68	27.30 $\pm$ 1.65	1.28 $\pm$ 0.08		

(Continued)

TABLE 1 | (Continued)

Isolate number	Locality of origin	Substrate type	Cell dimensions (mean ± SD)			Provisional morphospecies
			L (μm)	W (μm)	L/W ratio	
PA89	PLV		35.72 ± 2.41	26.94 ± 1.42	1.33 ± 0.07	<i>P. hoffmannianum</i>
PA90			37.81 ± 1.92	27.17 ± 1.40	1.39 ± 0.06	<i>P. lima</i>
PA91			46.88 ± 2.46	39.52 ± 1.47	1.19 ± 0.05	<i>P. hoffmannianum</i>
PA92			35.88 ± 1.55	28.15 ± 0.94	1.28 ± 0.07	<i>P. lima</i>
PA93			35.92 ± 1.46	26.68 ± 1.26	1.35 ± 0.05	
PA94			37.43 ± 1.95	26.82 ± 1.06	1.40 ± 0.07	
PA95			37.73 ± 1.42	27.40 ± 1.08	1.38 ± 0.05	
PA96			44.31 ± 2.87	36.47 ± 3.68	1.22 ± 0.11	<i>P. hoffmannianum</i>
PA97			35.14 ± 1.73	26.99 ± 2.93	1.31 ± 0.11	<i>P. lima</i>
PA98			34.58 ± 2.03	24.11 ± 1.35	1.44 ± 0.08	
PA99			36.69 ± 2.16	28.22 ± 1.32	1.30 ± 0.05	
PA100			36.31 ± 1.87	27.10 ± 1.17	1.34 ± 0.04	
PA101			36.85 ± 2.11	27.13 ± 2.53	1.36 ± 0.04	
PA102			36.53 ± 2.76	27.13 ± 2.10	1.35 ± 0.07	
PA103		34.70 ± 2.08	26.44 ± 1.94	1.31 ± 0.06		
PA104		37.06 ± 1.63	29.27 ± 1.80	1.27 ± 0.05		
PA20	PM	Attached buoy rope	28.28 ± 2.91	18.66 ± 2.25	1.52 ± 0.13	<i>P. rathymum</i>
PA26		<i>Sargassum</i> sp. (Ochrophyta)	36.93 ± 0.93	28.49 ± 1.02	1.30 ± 0.05	<i>P. lima</i>

Cell dimensions (mean ± SD) were determined from  $n = 30$  randomly selected cells after excluding obviously aberrant specimens.

BLP, BCS = Bahía de La Paz, Baja California Sur; AAR, VRS = Anegada de Adentro Reef, Veracruz Reef System, Veracruz; IV, VRS = Isla Verde, Veracruz Reef System, Veracruz; PLV, VRS = Piedra de La Virgen, Veracruz Reef System, Veracruz; PM = Puerto Morelos, Quintana Roo.

CA, United States); three to five clones per amplicon were sequenced using the M13 vector primers supplied with the kit. Sequencing was conducted with standard cycle sequencing chemistry ABI 3.1 (Applied Biosystems, Darmstadt, Germany). Sequencing products were analyzed on an ABI 3130 XL capillary sequencer (Applied Biosystems, Darmstadt, Germany) and the generated sequences were analyzed and assembled with CLC main workbench version 12.0.<sup>1</sup> The resulting sequences (Supplementary Table 1) were submitted to GenBank (Accession numbers: MZ308606-MZ308617 for the ITS, and MZ310155-MZ310171 for the LSU rDNA sequences).

### Molecular Taxonomic and Phylogenetic Analysis

Taxonomic sampling for phylogenetic analysis included representatives of *P. lima sensu lato* from most of its known global distribution. Sequences from strains labeled as *P. lima*, *P. hoffmannianum*, and *P. belizeanum* from the Americas, Asia, and Europe were retrieved from GenBank<sup>2</sup>. Sampling was restricted to LSU and ITS rDNA and most of the sequences were gathered from GenBank to be able to assemble a data set that included each locus from the same species. The respective rDNA loci of cultured isolates collected in Mexico, provisionally identified by light microscopy as referable to *P. lima sensu lato* and *P. hoffmannianum* (Table 1), were amplified, sequenced, and included in the alignment, yielding a full data set for phylogenetic analysis. Two data sets with 13 species were assembled, one for the LSU locus with 68 sequences, and another for the ITS

locus with 72 sequences (Supplementary Table 1). Taxonomic sampling mainly followed Chomérat et al. (2019), with the addition of recently described species in the genus (Luo et al., 2017; Nascimento et al., 2017; Lim et al., 2019). Each data set was analyzed with maximum likelihood and Bayesian inference approach under the same conditions as described below.

For each locus, multiple sequence alignment was performed independently in MAFFT 7.471 (Katoh and Standley, 2016) using the option *auto*, and visually inspected and corrected in Mesquite 3.61 (Maddison and Maddison, 2019), following suggestions by Morrison (2015). A Bayesian inference analysis was conducted in MrBayes 3.2.7 (Ronquist et al., 2012) through CIPRES web portal (Miller et al., 2010). Each locus was analyzed independently under the following conditions: nucleotide substitutions were modeled with a reversible jump approach (Huelsenbeck et al., 2004), allowing a mixture of models weighted by its posterior probability (PP) (Xie et al., 2011), rates heterogeneity was modeled with a gamma distribution (Yang, 1994; Huelsenbeck and Rannala, 2004), with four categories. The Monte Carlo Markov Chain was set to 10 million generations, with burning of 25%. For the specific case of ITS region, temperature was set to allow appropriate mixing. For both analysis, mixing and convergence were monitored in the output from MrBayes and in Tracer 1.7.1. (Rambaut et al., 2018).

Character support for clades was estimated with a non-parametric bootstrap (BS) (Felsenstein, 1985) in IQ-TREE 1.6.12 (Nguyen et al., 2014) using an ultrafast BS approach (Minh et al., 2013) with 1000 replicates. A Maximum Likelihood (ML) analysis was performed but only for support values. The ML analysis not only recovered the same branches, but the tree is the same for the

<sup>1</sup>www.CLCbio.com

<sup>2</sup>www.ncbi.nlm.nih.gov/genbank/

relevant nodes. The PP and BS values are quite similar; nodes with high PP have high BS support, yielding virtually the same results.

## Secondary Structure Modeling of Internal Transcribed Spacer Region 2 of Ribosomal RNA

The compensatory base change (CBC) approach was applied to investigate putative speciation among dinoflagellates based on potential hybridization barriers among isolates from the different clade deduced from the ITS/5.8S phylogeny (Gottschling and Plötner, 2004; John et al., 2014). The pattern of CBCs was determined from sequences of the representative isolates from Mexico from this study for each phylogenetic ITS/5.8S clade. These sequences were aligned with those of other taxa belonging to the PLSC with strains identified via BLAST searches in GenBank. The beginning and end of the ITS2 region in these strains were identified via homology with sequences of *P. lima* (GenBank accession FJ823582) retrieved from the ITS2 database (Koetschan et al., 2010), and were confirmed by comparison with a broader alignment of dinoflagellates. A multiple sequences alignment was performed from isolates collected from three regions in Mexico, as well as for representatives of clades III and IV. Sequences were aligned manually in Mesquite 3.61 (Maddison and Maddison, 2019). The ITS2 region was identified by molecular homology, and excised in a different file; the ITS2 segment lengths range from 156 to 186 bp.

The ITS2 secondary structure was predicted from the existing structural “a” model for the *Prorocentrum* ITS2 region (Koetschan et al., 2010), in agreement with the general dinoflagellate structures predicted by Gottschling and Plötner (2004). An identity matrix with a threshold of 20% was selected, with a sequence of *P. lima* retrieved from the same database as reference. The predicted structures were exported in an extended FASTA format; the CBCs in the predicted secondary structure were inspected in 4SALE (Seibel et al., 2006), and visualized using the Brucoleri algorithm (Brucoleri and Heinrich, 1988).

## Diarrhetic Shellfish Toxin Extraction and Analysis

### Toxin Extraction From *Prorocentrum* Cells

Cell pellets were extracted in 500  $\mu\text{L}$  50% methanol in FastPrep tubes, and after adding 0.9 g FastPrep lysing matrix D, were homogenized by reciprocal shaking in a FastPrep FP120 (Bio 101, Thermo Savant, Illkirch, France) at  $6.5 \text{ m s}^{-1}$  for 45 s. Homogenized samples were centrifuged at  $16,000 \times g$  for 15 min at  $11^\circ\text{C}$ . The supernatant from each sample was transferred into a  $0.45 \mu\text{m}$  pore-size spin-filter (Millipore Ultrafree, Eschborn, Germany) and centrifuged at  $11,000 \times g$  for 1.5 min at  $11^\circ\text{C}$ . Finally, filtrates were transferred into 2 mL LC-autosampler vials (Agilent, Waldbronn, Germany) for LC-MS/MS analysis.

### Toxin Analysis by Liquid Chromatography Coupled With Tandem Mass Spectrometry

The analytical system consisted of an SCIEX-4000 Q-Trap (Sciex, Darmstadt, Germany), triple quadrupole mass spectrometer equipped with a TurboSpray® interface coupled to an 1100

liquid chromatograph (LC) (Agilent, Waldbronn, Germany). The LC equipment included a solvent reservoir, in-line degasser (G1379A), binary pump (G1311A), refrigerated autosampler (G1329A/G1330B), and a temperature-controlled column oven (G1316A).

Separation of toxins was achieved following previous protocols (Krock et al., 2008; Nielsen et al., 2013) after injection of 5  $\mu\text{L}$  extract onto an analytical column packed with 3 mm Hyperclone™ 3  $\mu\text{m}$  BDS C8 130 Å  $50 \times 2 \text{ mm}$  (Phenomenex, Aschaffenburg, Germany), maintained at  $20^\circ\text{C}$ . The flow rate was  $0.2 \text{ mL min}^{-1}$  and gradient elution was performed by eluents A (water, formic acid, and ammonium formate) and B (acetonitrile, formic acid, and ammonium formate). Initial conditions were 12 min column equilibration with 5% B, followed by a linear gradient to 100% B in 10 min and isocratic elution until 16 min with 100% B. The program was then returned to initial conditions until 19 min (total run time: 31 min).

Detection of DSP toxin analogs was performed by LC-MS/MS by multiple reaction monitoring (MRM) experiments carried out in positive-ion mode with selected mass transitions (Supplementary Table 2). The following parameters were applied: curtain gas: 10 psi, CAD gas: medium, ion spray voltage: 5500 V, temperature: no heating, interface heater: on, declustering potential: 50 V, entrance potential: 10 V, exit potential: 15 V and dwell times of 100–200 ms per transition. Due to detection of a putative novel DTX1 isomer and associated diol-ester, provisionally dubbed DTX1a and DTX1a-D8, respectively, a collision-induced dissociation (CID) spectrum of DTX1 and the novel DTX1a compound was recorded in an enhanced product ion (EPI) mode of  $m/z$  836 (mass range  $m/z$  150–800) in the positive mode. Mass spectrometric parameters were the same as in the respective SRM experiments (Nielsen et al., 2013).

Analytical standards of okadaic acid (OA) ( $1 \text{ ng } \mu\text{L}^{-1}$ ), dinophysistoxin 1 (DTX1) ( $500 \text{ pg } \mu\text{L}^{-1}$ ), and dinophysistoxin 2 (DTX2) ( $500 \text{ pg } \mu\text{L}^{-1}$ ) from the Institute for Marine Biosciences, National Research Council, Halifax, NS, Canada were used to identify and quantify DSP toxins in extracts of *Prorocentrum* cells. Due to lack of standards for derivatives such as OA diol-ester (OA-D8) and dinophysistoxin 1-diol ester (DTX1-D8), cell quotas were expressed as OA and DTX1 equivalents, respectively, considering the following detection limits for OA ( $47 \text{ pg } \mu\text{L}^{-1}$ ), DTX1 ( $35 \text{ pg } \mu\text{L}^{-1}$ ), and DTX2 ( $25 \text{ pg } \mu\text{L}^{-1}$ ). Data acquisition and processing was performed with the Analyst Software Version 1.5, Sciex.

### Toxin Data Analysis

Statistical analysis of the toxin data was conducted with the software Infostat (V2019). Normality of toxin composition (OA, OA-D8, DTX1, DTX1-D8, DTX1a, and DTX1a-D8), cell toxin content, geographical localities (BLP, AAR, IV, and PLV) and different substrate types (Tracheophyta, Ochrophyta, Chlorophyta, Rhodophyta, and detritus) were examined by the Shapiro–Wilk test. Non-parametric analysis was performed on all the data sets because they did not show a normal distribution. The Wilcoxon–Mann–Whitney test was performed to determine differences in toxin composition among *P. lima* and *P. hoffmannianum* defined groups. Significant differences in

cell toxin content among groups (e.g., geographical localities and substrate types) were assessed with the Kruskal–Wallis test.

Ordination by principal components statistical analysis was performed using R version 4.1.0 (R Core Team, 2020; RStudio-Team, 2020). Prior to ordination analyses, relative toxin compositions were Hellinger-transformed using the *deconstand()* function of the package *vegan* (V2.5.7). Principal components of the dataset were calculated using the *prcomp()* function and plotted using the *ggbiplot* package (V0.55). Betadispersion (homogeneity of variance) of individual groups (i.e., based on locality of origin, clade and substrate type) was tested with the *betadisper()* function followed by permutational ANOVA (PERMANOVA) (Anderson, 2001) using the *adonis2()* function in *vegan*. Boxplots of differences in toxin compositions were visualized with the *ggplot2* package (V3.3.5).

## RESULTS

Several global biogeographical groups were defined based upon the location of origin of the isolates used for the morphological comparison and phylogenetic analysis of LSU and ITS rDNA sequence data for the PLSC and PHSC. These provisional groupings were established with reference to distributional regions for toxigenic benthic dinoflagellates from Latin America (Durán-Riveroll et al., 2019): Eastern Asian Pacific (China), Northeast Atlantic (Iberia, France), Mediterranean (Greece), Neotropical Southwest Atlantic (Brazil), Neotropical West Atlantic (Gulf of Mexico, Caribbean, Florida), Neotropical Pacific (Gulf of California, Mexico), and Tropical Australia. Not all biogeographical groups formed distinct clusters in the current analysis herein.

### Morphospecies Description and Identification

The illustrated *Prorocentrum* isolates from the coasts of Mexico (Figures 2, 3) can be categorized into one of three morphotypes: members of the PLSC, PHSC, or *P. rhathymum*. Cells of all PLSC isolates (Figures 2A–E, 3A–E) have a smooth thecal surface and the central area free of trichocyst pores, with slight differences in cell outline in lateral view and size as well as in shape and size of pores (round, oval, or bean-shaped). Slight differences in cell outline and size among PLSC isolates show infraspecific variation, rather than distinct characteristics of an individual strain. The PLSC isolates vary mainly in cell outline in thecal view. For example, PA78 cells are more rounded compared to other isolates, with a lower L/W ratio ( $1.21 \pm 0.04$ ) (Table 1). Cells of PA78 cells are the longest ( $46.36 \pm 1.33 \mu\text{m}$ ), but also show maximum width at or slightly behind the median line ( $38.36 \pm 1.36 \mu\text{m}$ ), whereas other illustrated PLSC isolates exhibit maximal width at 1/3 to 2/5 of the cell length toward the posterior end. Isolates PA48 (Figures 2D, 3D) and PA72 (Figures 2E, 3E) show a cell outline similar to PA8.

Cells of *P. hoffmannianum* also exhibit considerable morphological variation within the same clonal isolate. Variation in pore pattern similar to that among PLSC isolates can be also observed for *P. hoffmannianum* cells (Figures 2G,H), with more

densely scattered pores across the thecal surface and the central area free of pores; cells may be without (Figure 2G) or with (Figure 2H) a marginal row of pores. Numerous subcircular depressions are visible around the theca, creating a rough thecal surface. Some PLSC isolates and *P. hoffmannianum* cells reveal tiny depressions along the valve margins. Isolates PA70 and PA89 that belong to *P. hoffmannianum* show the cell outline (Figures 2G,H) and L/W ratio (1.21–1.33) (Table 1), characteristic of this species (Faust, 1990b). In Figures 3G–I, *P. hoffmannianum* isolates are depicted in right thecal and in right lateral-apical view, with Figure 3I showing a typical platelet arrangement and the two pores in the periflagellar area.

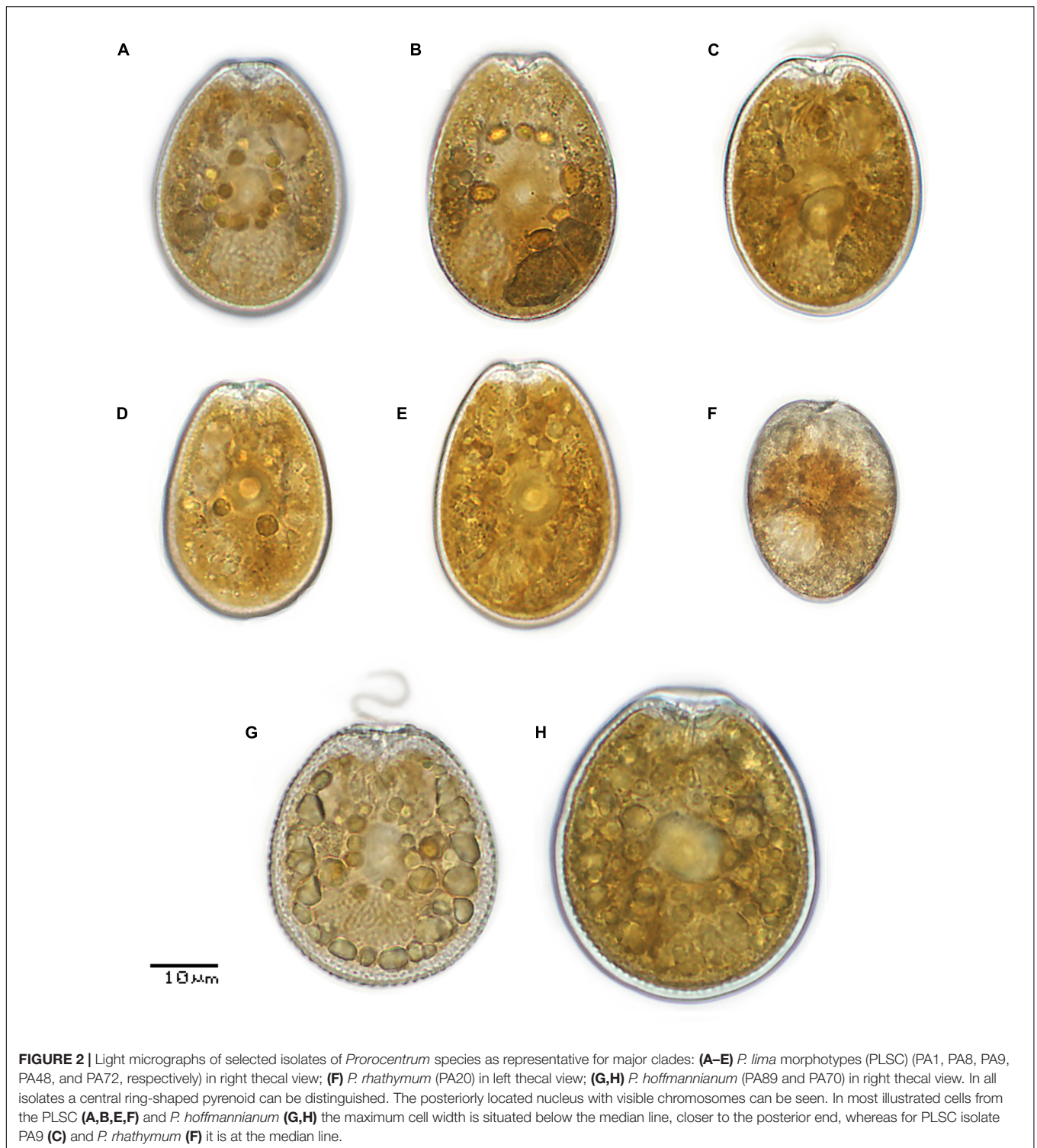
*Prorocentrum rhathymum* cells (PA20) have sparsely scattered double-rimmed trichocyst pores on a smooth thecal surface, tending to form radial rows at both sides of the posterior end and lacking in the subcentral area of the major thecal plates (Figures 2F, 3F). PA20 cells coincide with the original description of *P. rhathymum* (Loeblich et al., 1979), although in the illustrated cells in lateral view, the two major plates narrow slightly more to the posterior end than anteriorly. In many cells of the isolate this feature is absent, reflecting infraspecific variation.

### Molecular Genetics and Phylogeny

Separate multiple sequence alignments were produced for the ITS and LSU loci because there was little overlap between the sequences produced for both loci. We were only successful in amplifying and sequencing both loci for two strains from among the isolates from Mexico. We decided therefore not to perform a concatenated analysis with the two loci, but rather used the ITS alignment for further analysis. The ITS region is considered more informative in *Prorocentrum* at the infraspecific level and because it provides the opportunity of the opportunity for secondary structure analysis. In the present study, the higher intraspecific phylogenetic resolution and greater availability of reliable sequences focuses further discussion primarily on the ITS/5.8S region (Figure 4). Analysis for the LSU rDNA locus is also presented, but as **Supplementary Material** (shown in **Supplementary Table 1** and **Supplementary Figure 1**), and only for broad context and comparison with published literature.

A multiple sequences alignment, 670 bp in length, was produced for the ITS locus, including 72 sequences for the ITS/5.8 rDNA alignment, and 68 sequences for the LSU rDNA alignment (**Supplementary Table 1**). After 10 million generations of the Bayesian inference analysis, the average standard deviation of split frequencies was 0.003; chain swap values were satisfactory, with effective sample size 231 or above for all parameters. Convergence for both chains as well as mixing was considered satisfactory after inspection. Posterior probabilities (PP) and bootstrap (BT) values were drawn on the majority rule consensus produced with MrBayes.

Based upon ITS/5.8S rDNA sequences, representatives of *P. lima sensu lato* were recovered in five well supported clades (Figure 4), and the overall relationships between the five clades were well supported by PP and BT. Most isolates from Mexico were recovered in Clades I and II. Six isolates from this study are in Clade I, while three from PLV, Veracruz fall into Clade II with



isolates from Brazil. In any case, defined on the basis of ITS/5.8S sequences, Clade I does not exhibit global biogeographical consistency, as it includes strain representatives from China, Florida, and three distinct localities from Mexico.

On the ITS/5.8S rDNA tree, strains from Mexico in Clade II are all from PLV, Veracruz, but this clade also includes those

from geographically distant Brazil. Clades III and IV, both well supported, do not include any *Prorocentrum* isolates collected in Mexico, but exhibit higher congruence with geographical origin. Clade III comprises strains from China, whereas Clade IV includes those from the Northeast Atlantic (Iberia) and Mediterranean Sea. The remaining three isolates of the *P. lima*

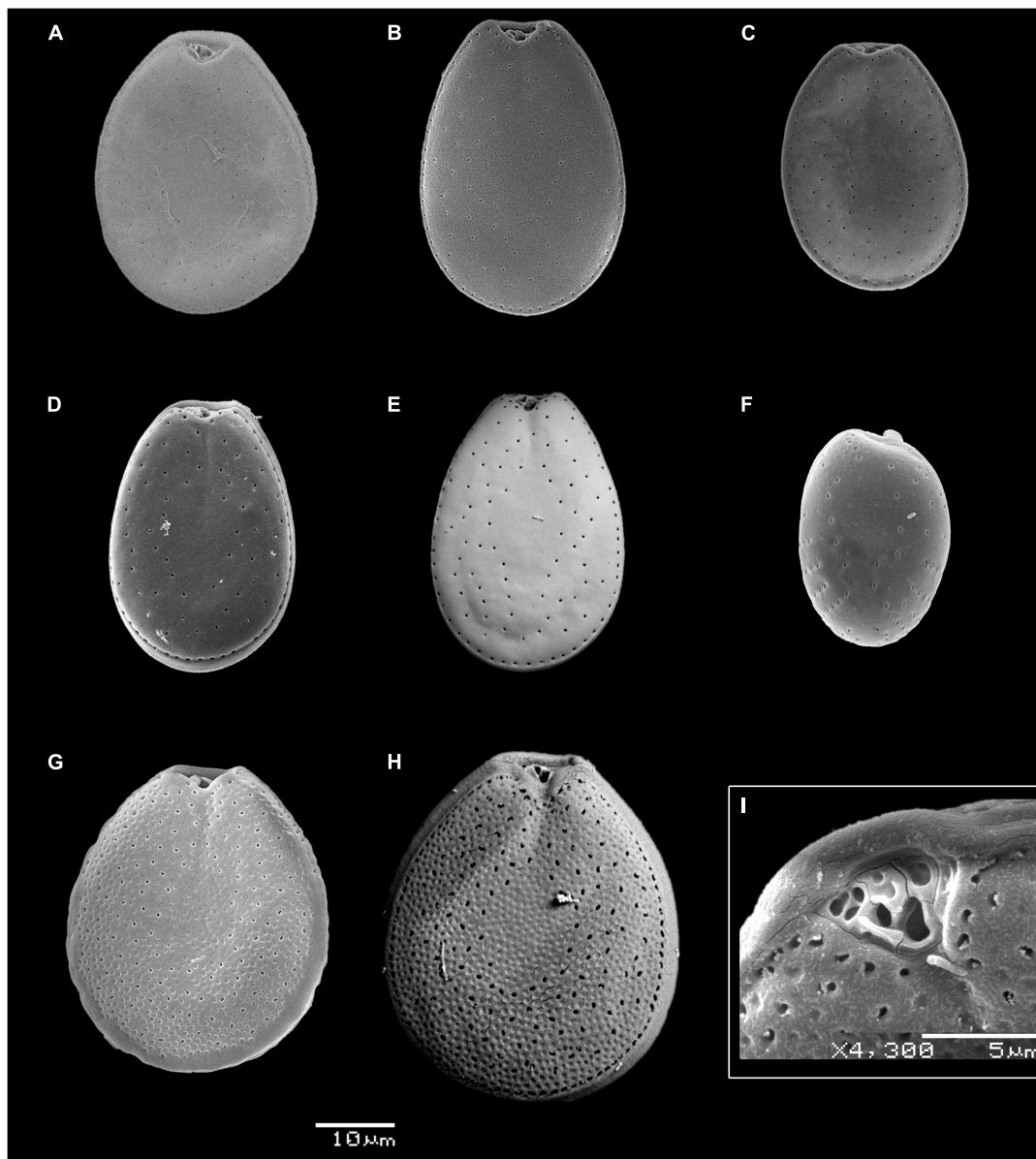


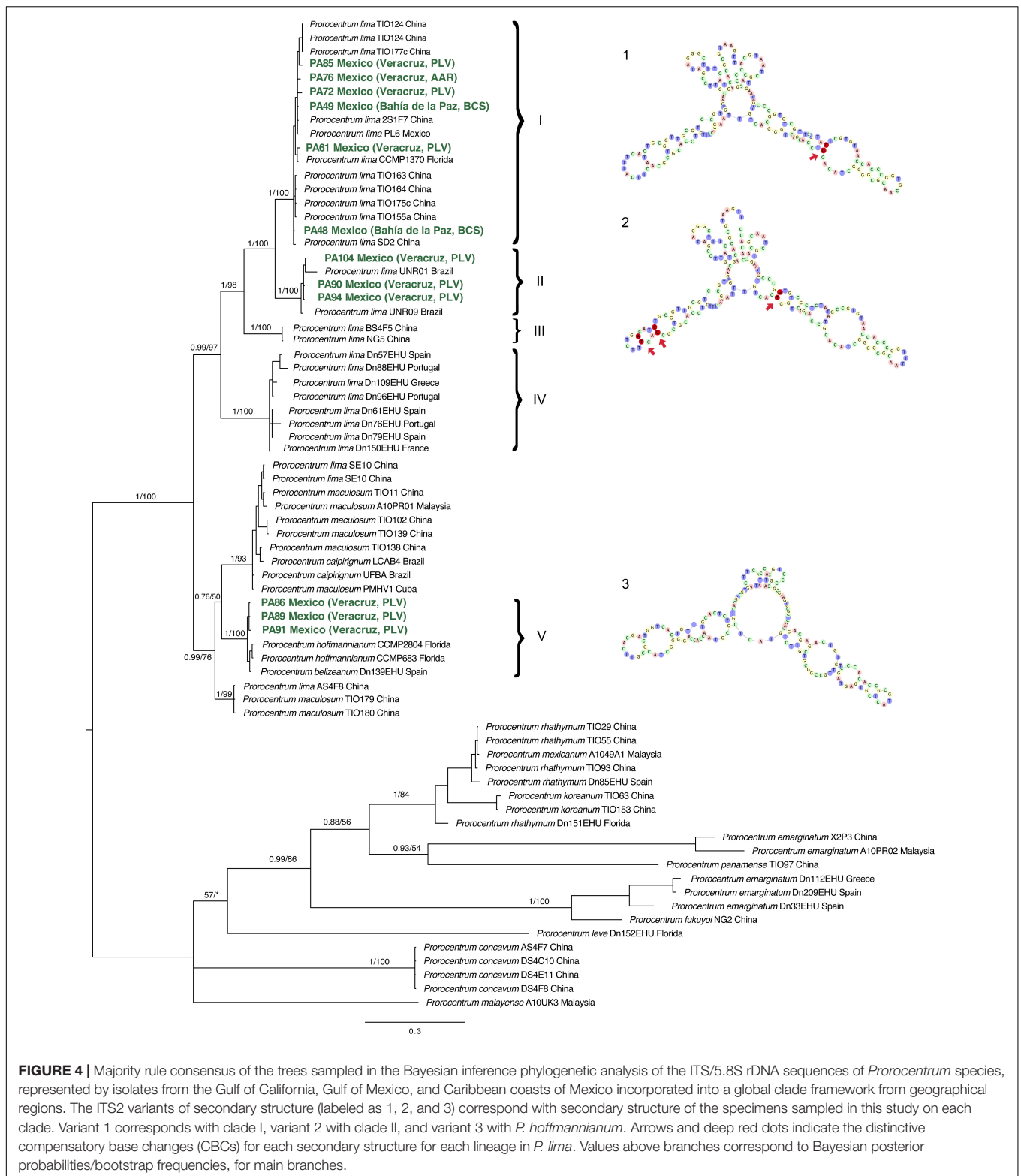
**FIGURE 3** | Scanning electron micrographs of selected isolates of *Prorocentrum* species as representative for major clades: **(A–E)** *P. lima* morphotypes (PLSC) (PA1, PA8, PA9, PA48, and PA72, respectively) in right view; **(F)** *P. rathymum* (PA20) in left thecal view; **(G–I)** *P. hoffmannianum* (PA89 and PA70); panels **(G,H)** in right thecal view; panel **(I)** in right lateral-apical view. Panel **(I)** shows a typical platelet arrangement and the two pores in the periflagellar area; numbering/lettering system for the platelets and pores in the periflagellar area: (e.g., ap–accessory pore, fp–flagellar pore) is according to Hoppenrath et al. (2013). Scale bars: 10  $\mu\text{m}$  in Panels **(A–H)** and 5  $\mu\text{m}$  in panel **(I)**.

*sensu lato* complex from PLV, Veracruz (PA86, PA89, and PA91) occur together with *P. hoffmannianum*/*P. belizeanum* morphotypes from Florida and Ibiza (western Mediterranean Sea), respectively, within Clade V, with two *P. lima* strains from China in its basal branches.

A multiple sequences alignment of 707 bp for 45 strains was produced from the LSU rDNA data set. After 10 million generations of the Bayesian inference analysis, the average standard deviation of the split frequencies was 0.004; effective sample size for all parameters was 234 or above. Convergence for

both chains as well as mixing was considered satisfactory after visual inspection in Tracer 1.7.1.

A comparison of the respective phylogenetic trees for ITS/5.8S rDNA (**Figure 4**) with LSU rDNA (**Supplementary Figure 1**) shows minor conflicts, but both trees are basically congruent. The topology of the phylogenetic tree based only on LSU rDNA sequences (**Supplementary Figure 1**) also recovers the same five clades as from ITS analysis, but relationships between clades are slightly different and poorly supported. The clade structure of the phylogenetic tree based only on LSU rDNA sequences also



groups strains from Brazil together with those from the Gulf of Mexico (primarily PLV, Veracruz), but those from China are widely distributed among clades. The association of *P. lima* PL6 from Isla El Pardito, Baja California Sur, Mexico forms a special

case. On the ITS/5.8 tree (Figure 4) it belongs in Clade 1 with the other PLSC members from Mexico but is situated with strains from China and a few others from Mexico in another clade on the LSU tree (Supplementary Figure 1).

The ITS sequences of strains from Mexico and the respective phylogenetic ITS2 clades exhibit a distinctive pattern of CBCs for their given ITS2 secondary structure (Figure 4 and Supplementary Figure 2). The ITS2 region consists of 156–186 bp in the *Prorocentrum* isolates from the coastal locations in Mexico (Supplementary Table 1). Within Clade I and Clade II, the strains from Mexico also fail to exhibit a clear geographical or morphological segregation, but compared to the basal Clade V, they do share a distinctive pattern of CBCs in their ITS secondary structure. Sequences from Clades I and II have distinctive structural patterns: Clade I members have a distinctive CBC at helix 3 (alignment positions C142 and G107), and sequences from Clade II have two CBCs at helix 2 (alignment positions A58 and T64, and C54 and G67) and one CBC at helix 3 (alignment position T95 and G155) (Figure 4 and Supplementary Figure 2). This distinctive pattern may be indicative of early stages of speciation.

## Toxin Composition and Cell Toxin Content

High variation in DSP toxin composition was exhibited among toxigenic clonal isolates ( $n = 67$  considering that 2 isolates were non toxigenic) from three disjunct geographical locations on the Gulf of California, Gulf of Mexico, and Caribbean coasts of Mexico. The only isolate of *P. rhathymum* (PA20) contained no detectable DSP toxins, but seven of the eight *P. hoffmannianum* isolates (all except PA71) were also toxigenic.

All isolates provisionally assigned to the PLSC (Table 1) produced substantial quantities of DSP toxins, readily detectable in methanolic extracts ( $ca. 6.7 \times 10^5$  cells  $mL^{-1}$ ) by LC-MS/MS (Figure 5). Confirmed toxin spectra by LC-MS/MS revealed the presence of six major analogs, including four well-known derivatives (OA, DTX) and their respective diol-esters (OA-D8, DTX1-D8), plus two novel DTX1 analogs (DTX1a, DTX1a-D8) of unconfirmed structure.

Among all *Prorocentrum* isolates, the following analogs were detectable in decreasing order of mean relative abundance: OA > OA-D8 > DTX1 > DTX1a > DTX1-D8 > DTX1a-D8. Toxin composition showed analogs OA, OA-D8, and DTX1 as the dominant toxins among PLSC and PHSC isolates. The relative toxin composition of OA, OA-D8, DTX1, DTX1a, and DTX1a-D8 were significantly higher for *P. lima* than for *P. hoffmannianum* isolates, but relative content of DTX1-D8 could not be distinguished between these species (total  $n = 67$ ,  $p < 0.05$ , Wilcoxon-Mann-Whitney test).

The two novel DTX analogs (DTX1a, DTX1a-D8) were stably produced among toxigenic isolates and readily detectable by LC-MS/MS analysis of toxin composition. Even without confirmed structures, they were therefore considered valid chemotaxonomic markers in the principal components analysis (PCA) (Figure 6) and PERMANOVA box-and-whisker plots of statistical significance (Figure 7). According to the PCA (Figure 6), the relative cell abundance (% molar) of DTX1 and minor novel variants DTX1a and DTX1a-D8 are strongly associated with isolates from Piedra de la Virgen, Veracruz Reef System (PLV, VRS), whereas high OA is characteristic of Isla Verde (IV, VRS) and Bahía de La Paz, Baja California Sur (BLP, BCS). The diol-ester analogs OA-D8 and DTX1-D8 are more prominent in isolates from Anegada de Adentro Reef (AAR, VRS) and BLP, BCS. Permutational multivariate analysis of variance (PERMANOVA in R, 999 permutations) comparison of relative toxin composition also shows differences between groups defined by locality of origin, ITS-defined clade, and substrate type, based on a pseudo F-statistic ( $*** \leq 0.0001$ ;  $** = 0.001$ ;  $* = 0.01$ ) (Figure 7).

Only isolates for which verified cell counts were available were selected for calculation of cell toxin content ( $fmol \text{ cell}^{-1}$ ) (Table 2 and Supplementary Figures 3A,B). For statistical analysis, isolates collected from detritus as dead Ochrophyta (Phaeophyceae) (PA46 and PA51) were considered to belong to both detritus and Ochrophyta groups, but the PM location

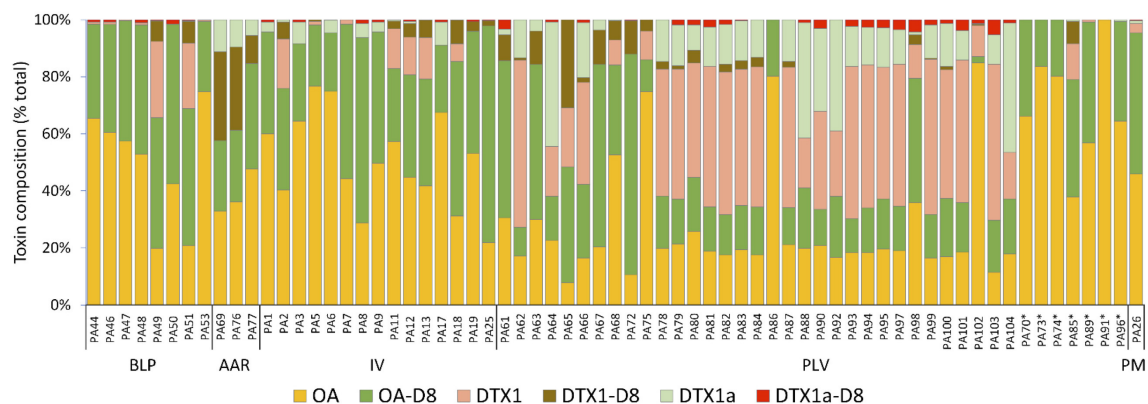
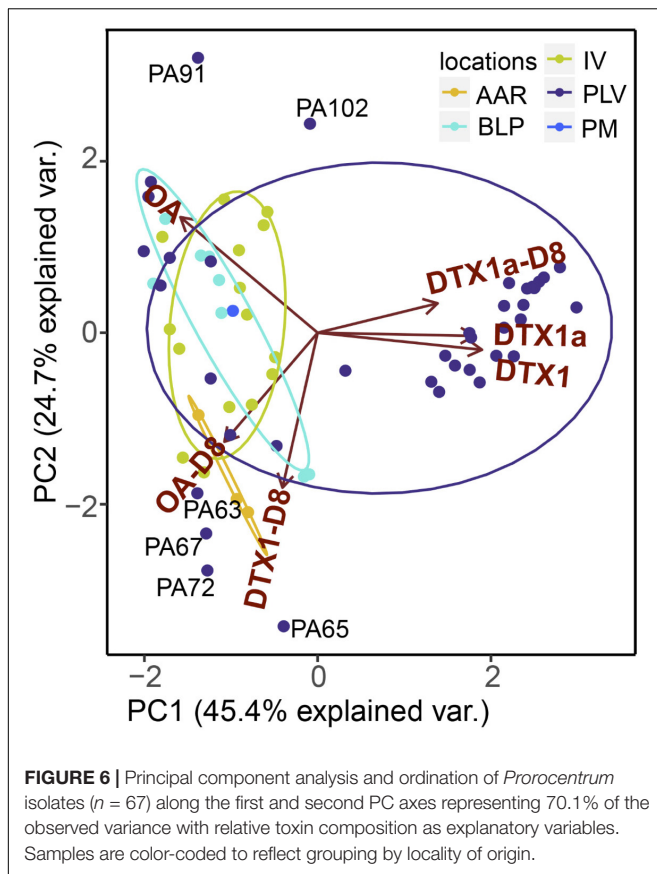


**FIGURE 5 |** Relative composition (% total) of DSP toxins (OA and DTX analogs) in isolates ( $n = 67$ ) of the *P. lima* complex (PLSC) and *P. hoffmannianum* (indicated by \*asterisk) from the Gulf of California, Gulf of Mexico, and Caribbean coasts of Mexico. BLP, BCS = Bahía de La Paz, Baja California Sur; AAR, VRS = Anegada de Adentro Reef, Veracruz Reef System, Veracruz; IV, VRS = Isla Verde, Veracruz Reef System, Veracruz; PLV, VRS = Piedra de La Virgen, Veracruz Reef System, Veracruz; PM = Puerto Morelos, Quintana Roo. Toxin acronym codes: OA = okadaic acid; OA-D8 = okadaic acid diol-ester; DTX1: dinophysistoxin 1; DTX1-D8 = dinophysistoxin 1 diol-ester; DTX1a = undescribed isomer of DTX1; DTX1a-D8: undescribed isomer of DTX1a-D8.



was excluded from the geographical comparison due to lack of replicate isolates ( $n = 1$ ). Among isolates morphologically belonging to the PLSC, the mean total cell toxin content among geographical localities (BLP  $n = 4$ , AAR  $n = 2$ , IV  $n = 10$  and PLV  $n = 2$ ) showed no significant differences ( $n = 18$ ,  $p < 0.05$ , Kruskal–Wallis test). Among epiphytic isolates collected from different substrate types, Tracheophyta ( $n = 7$ ), Ochrophyta ( $n = 6$ ), Chlorophyta ( $n = 3$ ), Rhodophyta ( $n = 3$ ), and detritus ( $n = 2$ ), there were no significant differences in toxin content ( $n = 21$ ,  $p < 0.05$ , Kruskal–Wallis test).

## DISCUSSION

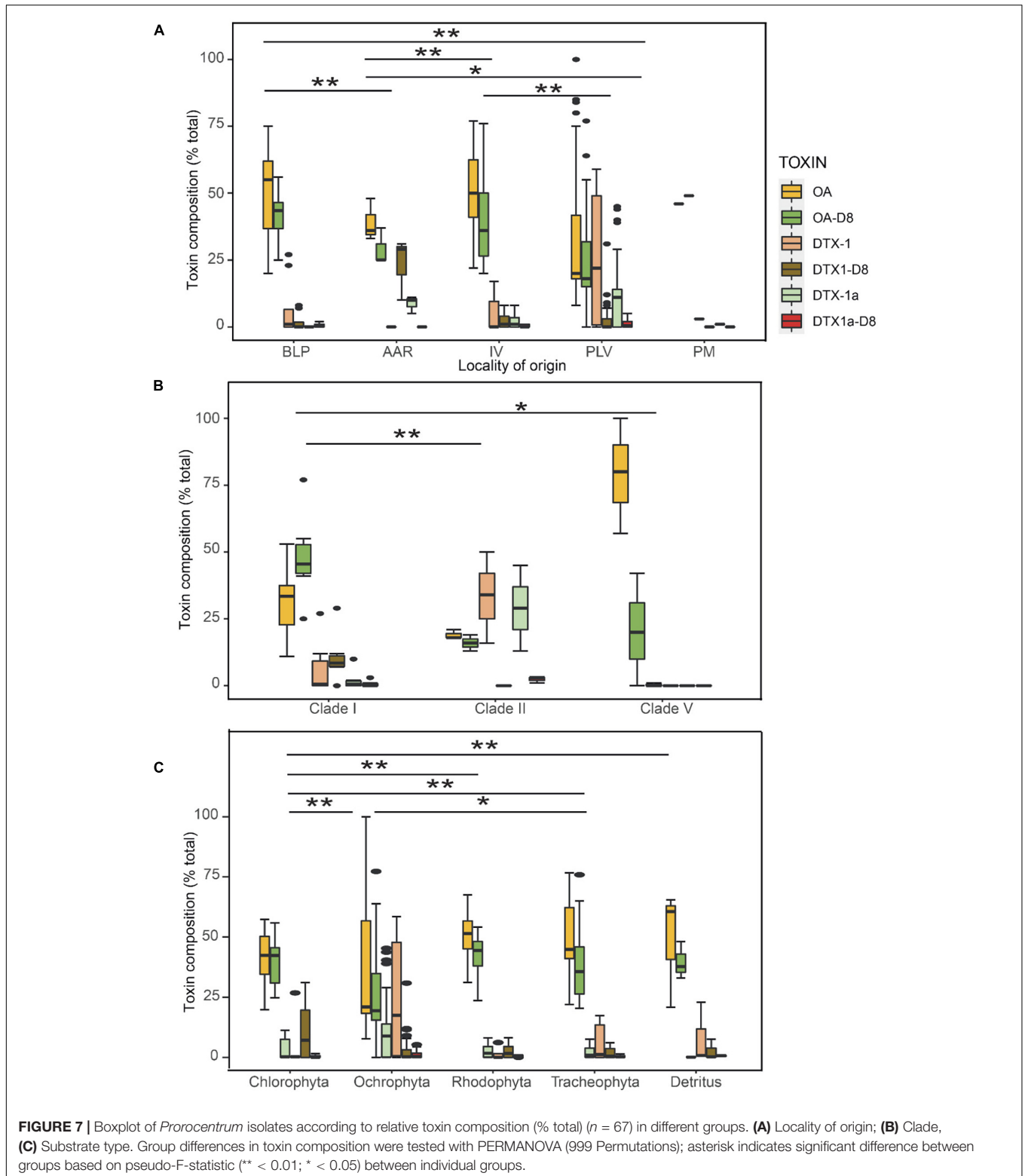
Membership in the PLSC has been defined originally on the basis of consistent morphological features, such as the smooth thecal surface, the structure of the periflagellar area and the presence of a central pyrenoid (Aligizaki, 2009). Within the genus *Prorocentrum* there remain several similar but unresolved taxa provisionally assigned to the PLSC as proposed by Aligizaki (2009) and subsequently revised with more molecular genetic support based on rDNA sequencing (Hoppenrath et al., 2014; Chomérat et al., 2019). Classification at the species level, however, is not always consistent between morphological vs. molecular genetic criteria. Early molecular studies of 18S rDNA gene sequences (Grzebyk et al., 1998) indicated the strong similarity between *P. lima* and *P. arenarium*, with only 11 nucleotide

substitutions between them and several shared synapomorphies. These congruencies led to classification of *P. arenarium* as a round *P. lima* morphotype (also later supported by Zhang et al. (2015)). *P. lima*, including *P. arenarium*, was proposed as monophyletic (Nagahama et al., 2011), but divided into several subclades correlated broadly to sample collection locations. No specific morphological characters were found to be related to any one subclade. Based on LSU and ITS/5.8S rDNA sequence phylogeny (Zhang et al., 2015) found very large infraspecific genetic differences in *P. lima* among five morphotypes from Hainan Island, South China Sea. All morphotypes fell within the morphological description of *P. lima* and *P. arenarium*, thereby leading to the conclusion that the morphological and molecular genetic data are contradictory.

Among and within defined benthic *Prorocentrum* species the high degree of phenoplasticity has certainly led to misidentifications. The presence of aberrant cells and multiple morphotypes varying in cell size, linear dimensions, number, and distributional patterns of thecal pores are frequently encountered in benthic *Prorocentrum* cultures, particularly in long-term ones (Y. Okolodkov, L. Durán-Riveroll, and A. Cembella, pers. observ.). The current analysis of cell size and shape variation among clonal cultures indicates that these are not generally reliable characteristics to distinguish among closely related species (e.g., *P. lima* vs. *P. hoffmannianum*) nor among infraspecific clones isolated from different substrate types or geographical locations within Mexican coastal waters. Faust (1990b), who originally described *P. hoffmannianum* from naturally collected specimens notes that cells of this species are typically larger and broader than those of *P. lima*. The cell size range (45–55  $\mu\text{m}$  long and 40–45  $\mu\text{m}$  wide) of *P. hoffmannianum* from Twin Cays, Belize is consistent with the dimensions of this species in cultures from Mexico, but the range is too broad to be diagnostic.

That such morphological variation can occur even in clonal cultures under standardized growth conditions in an apparently homogeneous environment indicates low constraints on expression of such key morphological features for taxonomic description based on autapomorphic criteria. If extrapolated to the natural benthic environment this may have led over-classification of morphotypes in some cases. On the other hand, the overall shape and structure characteristic of all benthic *Prorocentrum*, flattened heavily walled cells often adhering by mucus together as colonies upon substrates, are particularly adaptive for maximizing adhesion as epiphytes even under turbulent conditions and may provide barriers to grazing and space-competitors.

Such apparent contradictions between morphology and molecular genetic characteristics highlight the critical role of assessing cryptic speciation in defining diversity. There is indeed a high likelihood of cryptic speciation within “*P. lima* complex,” as originally suggested by Aligizaki (2009). In the current study of isolates from the three sub-regions of Mexico, all morphotypes consistent with *P. lima* are provisionally referred to the PLSC. In general, this follows the proposal by Aligizaki (2009) and recommendation by Hoppenrath et al. (2014), but with a minor amendment. The PLSC should be recognized



as a complex of individual species and not of infraspecific taxa within *P. lima sensu lato*. Hoppenrath et al. (2014) consider *Prorocentrum consutum* Chomérat et Nézan among species similar to *P. lima*. The lack of the *P. arenarium*

morphotype from the sampling in Mexico does not allow us to resolve its distinction from *P. lima*. We therefore consider them synonymous, following Nagahama et al. (2011), Hoppenrath et al. (2014), and Lassus et al. (2016). A recently

**TABLE 2** | Cell content of DSP toxins (OA and DTX plus analogs) from cultured benthic *Prorocentrum* isolates assigned to the *P. lima* complex (PLSC).

Isolate	Cell toxin (fmol cell <sup>-1</sup> )						Total toxin
	OA	OA-D8	DTX1	DTX1-D8	DTX1a	DTX1a-D8	
PA2	6.37	5.60	2.70	0.91	0.13	ND	15.71
PA3	10.12	4.25	ND	ND	1.18	0.12	15.66
PA5	3.22	0.91	0.05	0.02	ND	ND	4.20
PA6	23.82	6.49	ND	ND	1.38	0.07	31.76
PA8	12.77	28.82	0.00	ND	2.11	0.61	44.31
PA11	4.74	2.11	1.13	0.22	0.03	0.01	8.24
PA17	21.83	7.63	ND	ND	2.57	0.26	32.29
PA18	2.40	4.17	0.47	0.62	0.02	ND	7.68
PA19	6.60	5.30	ND	0.40	ND	0.09	12.39
PA25	4.88	16.97	ND	0.43	ND	0.05	22.34
PA26	13.89	14.96	1.01	ND	0.30	0.08	30.24
PA46	20.23	12.61	0.27	ND	0.03	0.25	33.39
PA47	11.98	8.83	0.05	ND	ND	ND	20.86
PA51	7.13	16.49	7.71	2.56	0.09	0.13	34.09
PA53	23.10	7.61	0.15	ND	0.03	ND	30.89
PA69	6.51	4.92	ND	6.05	2.20	ND	19.69
PA75	17.31	2.58	2.30	0.89	ND	ND	23.07
PA77	3.63	2.81	ND	0.75	0.41	ND	7.60
PA86	9.31	2.30	ND	ND	ND	ND	11.61

Only selected *Prorocentrum* isolates ( $n = 19$ ) with verified cell counts and quantifiable toxins well above the detection limit are included (ND = not detected or below nominal quantitation limit). OA = okadaic acid; OA-D8 = okadaic acid diol-ester; DTX1: dinophysistoxin 1; DTX1-D8 = dinophysistoxin 1 diol-ester; DTX1a = undescribed isomer of DTX1; DTX1a-D8: undescribed isomer of DTX1-D8.

described species from Brazil, *Prorocentrum caipirignum* S. Fraga, M. Menezes et S. Nascimento, is similar to *P. lima* in its morphology, and appears close to the clades of *P. lima* and *P. hoffmannianum* in previous phylogenetic trees based on ITS and LSU rDNA sequences (Nascimento et al., 2017). No morphotypes consistent with *P. caipirignum* were found among populations studied from Mexico, but this species was included in the ITS and LSU-based phylogenetic alignments herein, and the close relationship with the PLSC was confirmed.

Noting the uncertainty in the species boundaries between *P. hoffmannianum* and *P. belizeanum*, Hoppenrath et al. (2013) would also include *Prorocentrum sabulosum* M. A. Faust and *Prorocentrum tropicale* M. A. Faust in the PHSC. According to Herrera-Sepúlveda et al. (2015), *P. lima sensu lato* is a sister to the *P. hoffmannianum/P. belizeanum/P. maculosum* group. This phylogenetic analysis concludes that *P. belizeanum* M. A. Faust is conspecific with *P. hoffmannianum*, forming a highly supported monophyletic clade within the PHSC, but with three subclades broadly corresponding to the sample collection regions. Our current phylogenetic analysis support the paraphyly of the PLSC, wherein the PHSC with its autapomorphic feature forms a monophyletic subclade of Clade 5 (Figure 4 and Supplementary Figure 1; and see Chomérat et al. (2019).

Based on SSU rDNA analysis, *P. hoffmannianum*, *P. belizeanum*, and *P. maculosum* comprise a highly supported monophyletic group (Herrera-Sepúlveda et al., 2015). *P. maculosum* M. A. Faust is also morphologically very similar to

members of the PLSC and *P. hoffmannianum* (Hoppenrath et al., 2013), and hence was concurrently misidentified as *P. concavum* (Glibert et al., 2012). This species is considered to be a sister group to the *P. hoffmannianum/P. belizeanum* clade.

*Prorocentrum rhathymum* is morphologically distinct from both the PLSC and PHSC, but still remains an enigma. Often considered a synonym of *P. mexicanum* B. F. Osorio (Steidinger and Tangen, 1996; Faust and Gulledege, 2002), *P. rhathymum* and *P. mexicanum* have also been recognized as distinct species (Cortés-Altamirano and Sierra-Beltrán, 2003), based on both morphological and ecological (habitat) differences. Phylogenetic analysis of strains from Florida (An et al., 2010) supports this separation. On the contrary, molecular characterization of Korean strains and their comparison with other *P. rhathymum* and *P. mexicanum* strains from different geographical regions did not allow Lim et al. (2013) to classify them as separate species. Molecular phylogenetic analysis of *P. rhathymum* strains from Florida (An et al., 2010) vs. *P. cf. rhathymum* from Korea has served to highlight inconsistencies in species level discrimination (Lim et al., 2013) and has led to embedding these groups in the paraphyletic PLSC clade (Chomérat et al., 2019).

A comparison of the respective phylogenetic trees for ITS/5.8S rDNA (Figure 4) with LSU rDNA (Supplementary Figure 1) shows minor conflicts but both are basically in congruence with the literature on species associations within *Prorocentrum* [e.g., Chomérat et al. (2019)]. Nevertheless, comparative analysis of the LSU sequences (Supplementary Figure 1) among new strains from geographically distant sub-tropical locations (Gulf of Mexico, Caribbean and Gulf of California) integrated with global strains of benthic *Prorocentrum* species does not clearly resolve the PLSC at the species level. This remains paraphyletic and does not show clear geographical separation among the clades. The topology of the ITS/5.8S rDNA phylogenetic tree (Figure 4) recovered is generally congruent with previous molecular phylogenetic analyses of the PLSC and association with *P. hoffmannianum* and allies, but with minor differences. A Maximum Likelihood (ML) analysis based on an LSU rDNA matrix of *Prorocentrum* species (Chomérat et al., 2019) shows the PHSC in a tight cluster within the PLSC node/clade. Again, in all phylogenetic analyses the PLSC appears to be paraphyletic and the *P. hoffmannianum* group (PHSC) branches after some basal *P. lima* isolates (Figure 4 and Supplementary Figure 1) and is consistent with the scheme published in Chomérat et al. (2019).

Although we are aware that there is still limited and perhaps not representative sampling coverage of genotypes from the different target regions, reference to the ITS/5.8S sequences rather than LSU successfully resolves some of the issues regarding the scope of the PLSC and cryptic speciation. Nevertheless, there are also intriguing anomalies to consider from the perspective of biogeographical origins. Benthic dinoflagellates, including epiphytic *Prorocentrum* are typically rather sessile and tend to remain associated with the local substrate (Durán-Riveroll et al., 2019). In principle, this suggests that endemic populations have reduced potential for genetic exchange with geographically disjunct populations of emerging species. Knowledge of the sexual life history stages of benthic *Prorocentrum* is extremely limited, and recombination events

are rarely observed (unlike for the phylogenetically distinct planktonic species). Putative sexual (resting) cysts have been reported for *P. lima* (Faust, 1993; Faust et al., 1999) and another benthic species *Prorocentrum marinum* (Cienkowski) Steidinger et Williams ex Head (Faust, 1990a, 1993), but these reports are typically inferences from morphological analysis of field specimens rather than confirmed from mating and germination studies. In fact, true fossilizable sexual resting cysts have just recently been confirmed for the first time and in only one species, *Prorocentrum leve* M.A. Faust, Kibler, Tester et Litaker (Mertens et al., 2017). Circumstantial evidence therefore suggests that sexual recombination events may be rather rare within endemic benthic populations.

Potential hybridization barriers appear within the PLSC (Clade I–V) including the PHSC (Clade V). Indeed, the segregation of *P. hoffmannianum* in Clade V indicates clear speciation and is consistent with the morphological differentiation and divergence from *P. lima*. Patterns of micro-ecological niche differentiation cannot, however, be inferred from substrate type or local biogeographical barriers. Arguments for cryptic speciation could be interpreted from the existence of hybridization barriers by the presence of CBCs by pairwise comparisons in the ITS2 region between the clades (Figure 4), as supported by several independent studies (Fabry et al., 1999; Coleman, 2003, 2009; John et al., 2014). Though not mechanistically linked to the development of either pre- or post-zygotic incompatibility, when present, CBCs or hemi-CBCs consistently correlate with species-level divergences even among closely related lineages (Gottschling and Plötner, 2004; Gottschling et al., 2005; John et al., 2014). Not all speciation events, however, lead to the development of CBCs or hemi-CBCs. Consequently, the lack of CBCs between clades should not be interpreted as evidence against their being separate species. Direct evidence of speciation events based on cyst unviability are missing, but the accumulation of CBCs within Clades I–III indicates at least cryptic speciation is in progress.

An additional caveat in interpretation of “speciation” in *Prorocentrum* is related to morphotaxonomic and nomenclatorial uncertainties, particular with the older literature on species descriptions. For example, in the current analysis, *P. belizeanum* is included in Clade V with *P. hoffmannianum* and some basal *P. lima*. As the name implies, *P. belizeanum* was described originally from Belize; its current distribution appears to be restricted to the Caribbean region (GBIF.Org, 2020). The inclusion of *P. belizeanum* Dn139EHU from Spain (as reported in GenBank) may therefore simply represent an original misidentification or more likely the fact that they are synonyms (Herrera-Sepúlveda et al., 2015), as also supported by the tight association in Clade V.

Biogeographical distributional patterns and substrate associations are key to understanding population dynamics and speciation among benthic *Prorocentrum*. No definitive association have been identified in temperate areas (Foden et al., 2005), whereas in tropical environments this genus has been preferentially associated with both filamentous turf (Parsons and Preskitt, 2007) and Phaeophyceae (Delgado et al., 2006) as substrates. The current analysis of morphotypes, rDNA-defined

genotypes and toxin chemotypes failed to yield clear patterns dependent upon substrate types or biogeographical locations in Mexican coastal waters. Nevertheless, the clustering of *Prorocentrum* genotypes belonging to the PLSC from the eastern North Atlantic coast and the western Mediterranean Sea (Ibiza) within Clade II on the ITS/5.8S rDNA tree, and similar clustering on the LSU rDNA tree, do indicate a biographical barrier to genetic exchanges with Caribbean and Gulf of Mexico populations. On the other hand, benthic *Prorocentrum* species are notorious for and commonly found rafting upon detritus and detached macroalgae (Bomber et al., 1988; Faust et al., 1999) – a viable means of long distance dispersal by ocean currents. Based upon ITS/5.8S rDNA analysis, strains in Clade II are from one locality in Mexico (Veracruz, PLV), but this clade also includes a strain from geographically distant Brazil. Admittedly speculative, but mixing of genotypes may have occurred via rafting from the Brazilian coast by entrainment in the northwestward flow of the Atlantic South Equatorial Current linked to the Guiana Current and eventually transfer to the Gulf of Mexico in the Caribbean Current. Similarly, the close ITS genotypic association of *P. hoffmannianum* from the Gulf of Mexico and the Florida coast in Clade V may be plausibly explained by prevailing current transport of detritus and macroalgae bearing *Prorocentrum* epiphytes.

High chemodiversity in toxin composition was evident among *Prorocentrum* species and isolates differing in geographical origin, substrate type and clade assignment. In fact, clonal variation in toxin composition was substantially greater than as defined by morphological or molecular genetic criteria such as ITS/5.8S sequences. Since these toxin profiles are stable yet distinct under homogeneous culture conditions and throughout the culture cycle, this provides the opportunity to define genetically fixed chemotaxonomic markers. To our knowledge the current study represents the largest comparison ( $n = 67$  isolates) of toxin compositional profiles among populations for any genus of marine benthic dinoflagellate. Despite this large data set, we were unable to confirm clear distinctions among substrates or geographical origins to define populations within a species. Between species *P. lima* and *P. hoffmannianum* there were apparent tendencies for toxin compositional differences for some analogs (OA, OA-D8, DTX1, DTX1a, and DTX1a-D8) but not for others (DTX1-D8). There were no statistical differences between these species in total toxin content. The toxin compositional data support the contention that production of DSTs is likely an obligate trait within the PLSC *sensu stricto* (Chomérat et al., 2019). Close relatives of *P. lima*, such as *P. caipirignum* (previously as *P. cf. maculosum*) (Yasumoto et al., 1984; Hu et al., 2017; Luo et al., 2017) from diverse populations from Malaysia (Lim et al., 2019), the South China Sea (Luo et al., 2017), and Brazil (Nascimento et al., 2017), have also been found as consistently toxigenic. Nevertheless, at this stage it is premature to conclude that this high chemodiversity can be effectively applied to distinguish genotypes or “species,” in the absence of knowledge on the biosynthetic gene clusters for these polyketides.

This multivariate study of diversity of benthic *Prorocentrum* yields valuable insights into the processes of incipient speciation

and definition of appropriate taxonomic markers and criteria for distinguishing species. Sexual life histories are lacking for most benthic dinoflagellates, and particularly for *Prorocentrum* species. Molecular genetic markers are usually capable of discriminating “benthic,” “tychoplanktonic,” and “planktonic” taxa, but provide only a static view of behavior and species interactions. Only by combining comparative approaches to morphotaxonomy, breeding affinities, inheritance of toxigenicity and molecular diversity within and among global population will it be feasible to define the ecological niches and adaptive strategies to account for the survival and success of benthic dinoflagellate species. Such multidisciplinary approaches are necessary to distinguish the mechanisms among those of phylogenetically close relatives in planktonic assemblages.

## DEDICATION

This publication is dedicated to the memory of our dear friend and colleague Maria A. Faust (21 April 1930–24 April 2021), recently deceased after a 40-year career at the National Museum of Natural History within the Smithsonian Institution (Washington, DC, United States). She was a true pioneer in biodiversity research, particularly on tropical marine dinoflagellates, discovering and describing dozens of new benthic species including many *Prorocentrum* discussed herein.

## DATA AVAILABILITY STATEMENT

The datasets presented in this study can be found in online repositories. Alignments available upon request. The names of the repository/repositories and accession number(s) can be found in the article/**Supplementary Material**.

## AUTHOR CONTRIBUTIONS

LD-R and AC conceived the project, designed the field and laboratory studies in consultation with YO, extracted and prepared the rDNA for LSU and ITS sequencing, contributed equally, and led and coordinated the drafting of the manuscript. LD-R, AC, and YO conducted the field sampling for epibenthic dinoflagellates. LD-R prepared the preliminary isolates for culture and maintained the clonal strains at ICMyL-UNAM, Mexico, and LD-R, UT-J, and AC at AWI, Germany. UJ supervised the rDNA gene sequencing and together with RG-S conducted the phylogenetic and molecular taxonomic analysis. LD-R and YO conducted the morphotaxonomic analysis of *Prorocentrum* isolates. UT-J performed the toxin extractions for

LC-MS/MS of DSP toxins and data analysis under supervision from BK. CH with AC and UJ performed the statistical analyses of environmental, toxin, and phylogenetic data. All authors contributed actively to the preparation of data content and writing of this manuscript.

## FUNDING

This research was funded primarily by the Consejo Nacional de Ciencia y Tecnología (CONACyT, Mexico) Basic Science Project, number A1-S-8616 awarded to LD-R. Financial contribution for the preparation and publication of this manuscript and also associated research activities was provided to AC, BK, and UJ within the Helmholtz research program “Changing Earth, Sustaining our Future” (Sub-topic 6.2 Adaptation of marine life) of the Alfred-Wegener-Institut, Helmholtz-Zentrum für Polar- und Meeresforschung, Germany. The Deutscher Akademischer Austauschdienst (DAAD) made possible the research stay of LD-R at AWI, with focus on the molecular biological aspects. UT-J acknowledges the funding support from the International Max Planck Research School of Marine Microbiology for her master studies and research opportunities.

## ACKNOWLEDGMENTS

We thank Manuel Victoria-Muguirra of *Dorado Buceo* for boat access and logistical support with field sampling from Veracruz, and Manuel Rodríguez-Gómez from the Acuario de Veracruz for donating filtered seawater. Mario Fernando Sánchez Bernal was responsible for imaging and curation. Laura Elena Gómez-Lizárraga from the Scanning Electron Microscopy Laboratory at Instituto de Ciencias del Mar y Limnología, Universidad Nacional Autónoma de México (ICMyL-UNAM) provided micrographs; Manuel E. Martínez-Cruz, Hugo Pérez-López, and Apatzingán Palomino-Hermosillo assisted with SEM sample preparation and cell measurements; Andrea García-Casillas (UNAM) performed statistical data analysis. Technical assistance of Annegret Müller and Thomas Max for LC-MS/MS analysis of DSP toxins and Lena Nieke for *Prorocentrum* culture maintenance at AWI is much appreciated.

## SUPPLEMENTARY MATERIAL

The Supplementary Material for this article can be found online at: <https://www.frontiersin.org/articles/10.3389/fmars.2021.716669/full#supplementary-material>

## REFERENCES

- Aguilar-Trujillo, A. C., Okolodkov, Y. B., Herrera-Silveira, J. A., Merino-Virgilio, F. D. C., and Galicia-García, C. (2017). Taxocoenosis of epibenthic dinoflagellates in the coastal waters of the northern Yucatan Peninsula before and after the harmful algal bloom event in 2011–2012. *Mar. Pollut. Bull.* 119, 396–406. doi: 10.1016/j.marpolbul.2017.02.074
- Aligizaki, K. (2009). “Spread of potentially toxic benthic dinoflagellates in the Mediterranean Sea: a response to climate change?,” in *Phytoplankton Response to Mediterranean Environmental Change*, ed. C. Workshop (Tunisia: CIESM), 57–61.
- Almazán-Becerril, A., Escobar-Morales, S., Rosiles-González, G., and Valadez, F. (2015). Benthic-epiphytic dinoflagellates from the northern portion of the Mesoamerican reef system. *Bot. Mar.* 58, 115–128. doi: 10.1515/bot-2014-0093

- An, T., Winshell, J., Scorzetti, G., Fell, J. W., and Rein, K. S. (2010). Identification of okadaic acid production in the marine dinoflagellate *Prorocentrum rhathymum* from Florida Bay. *Toxicol.* 55, 653–657. doi: 10.1016/j.toxicol.2009.08.018
- Anderson, M. J. (2001). A new method for non-parametric multivariate analysis of variance. *Austral. Ecol.* 26, 32–46. doi: 10.1111/j.1442-9993.2001.01070.pp.x
- Barón-Campis, S. A., Okolodkov, Y. B., Ríos-Lara, G. V., Vázquez-Gómez, N., Rubio-Sánchez, V., Arce-Rocha, G., et al. (2014). “Dinoflagelados nocivos y ciguatoxinas en la costa norte de Yucatán: un riesgo para el futuro desarrollo de la maricultura,” in *Proceedings of the XXI Congreso Nacional de Ciencia y Tecnología del Mar*, Cozumel, Quintana Roo, Mexico.
- Blackburn, S. I., Bolch, C. J. S., Haskard, K. A., and Hallegraeff, G. M. (2001). Reproductive compatibility among four global populations of the toxic dinoflagellate *Gymnodinium catenatum* (Dinophyceae). *Phycologia* 40, 78–87. doi: 10.2216/i0031-8884-40-1-78.1
- Boisnoir, A., Pascal, P.-Y., Cordonnier, S., and Lemée, R. (2019). Spatio-temporal dynamics and biotic substrate preferences of benthic dinoflagellates in the Lesser Antilles, Caribbean sea. *Harmful Algae* 81, 18–29. doi: 10.1016/j.hal.2018.11.012
- Bomber, J. W., Morton, S. L., Babinchak, J. A., Norris, D. R., and Morton, J. G. (1988). Epiphytic dinoflagellates of drift algae—another toxigenic community in the ciguatera food chain. *Bull. Mar. Sci.* 43, 204–214.
- Brucoleri, R. E., and Heinrich, G. (1988). An improved algorithm for nucleic acid secondary structure display. *Bioinformatics* 4, 167–173. doi: 10.1093/bioinformatics/4.1.167
- Chomérat, N., Bilien, G., and Zentz, F. (2019). A taxonomical study of benthic *Prorocentrum* species (Prorocentrales, Dinophyceae) from Anse Dufour (Martinique Island, eastern Caribbean Sea). *Mar. Biodivers.* 49, 1299–1319. doi: 10.1007/s12526-018-0913-6
- Coleman, A. W. (2003). ITS2 is a double-edged tool for eukaryote evolutionary comparisons. *Trends Genet.* 19, 370–375. doi: 10.1016/s0168-9525(03)00118-5
- Coleman, A. W. (2009). Is there a molecular key to the level of “biological species” in eukaryotes? A DNA guide. *Mol. Phylogenet. Evol.* 50, 197–203. doi: 10.1016/j.ympev.2008.10.008
- Cortés-Altamirano, R., and Sierra-Beltrán, A. P. (2003). Morphology and taxonomy of *Prorocentrum mexicanum* and reinstatement of *Prorocentrum rhathymum* (Dinophyceae). *J. Phycol.* 39, 221–225. doi: 10.1046/j.1529-8817.2003.01112.x
- Delgado, G., Lechuga-Devéze, C. H., Popowski, G., Troccoli, L., and Salinas, C. A. (2006). Epiphytic dinoflagellates associated with ciguatera in the northwestern coast of Cuba. *Rev. Biol. Trop.* 54, 299–310. doi: 10.15517/rbt.v54i2.13870
- Durán-Riveroll, L. D., Cembella, A. D., and Okolodkov, Y. B. (2019). A review on the biodiversity and biogeography of toxigenic benthic marine dinoflagellates of the coasts of Latin America. *Front. Mar. Sci.* 6:148.
- Fabry, S., Köhler, A., and Coleman, A. W. (1999). Intraspecific analysis: comparison of ITS sequence data and gene intron sequence data with breeding data for a worldwide collection of *Gonium pectorale*. *J. Mol. Evol.* 48, 94–101. doi: 10.1007/pl00006449
- Faust, M. (1993). “Sexuality in a toxic dinoflagellate, *Prorocentrum lima*,” in *Toxic Phytoplankton Blooms in the Sea*, eds T. J. Smayda and Y. Shimizu (New York: Elsevier Science Publishing Co), 121–126.
- Faust, M. A. (1990b). Morphologic details of six benthic species of *Prorocentrum* (Pyrrophyta) from a mangrove island, Twin Cays, Belize, including two new species. *J. Phycol.* 26, 548–558. doi: 10.1111/j.0022-3646.1990.00548.x
- Faust, M. A. (1990a). “Cysts of *Prorocentrum marinum* (Dinophyceae) in floating detritus at Twin Cays, Belize mangrove habitats,” in *IV International Conference on Toxic Marine Phytoplankton*, eds E. Granéli, B. Sundström, L. Edler, and D. M. Anderson (Lund: Elsevier), 138–143.
- Faust, M. A., and Gullede, R. A. (2002). Identifying harmful marine dinoflagellates. *Contr. U.S. Natl. Herb.* 42, 1–144.
- Faust, M., Larsen, J., and Moestrup, Ø (1999). *ICES Identification Leaflets for Plankton (Leaflet No. 184): Potentially Toxic Phytoplankton. 3. Genus Prorocentrum (Dinophyceae)*. Copenhagen: International Council for the Exploitation of the Sea.
- Felsenstein, J. (1985). Confidence limits on phylogenies: an approach using the bootstrap. *Evolution* 39, 783–791. doi: 10.2307/2408678
- Foden, J., Purdie, D. A., Morris, S., and Nascimento, S. (2005). Epiphytic abundance and toxicity of *Prorocentrum lima* populations in the Fleet Lagoon, UK. *Harmful Algae* 4, 1063–1074. doi: 10.1016/j.hal.2005.03.004
- Fritz, L., and Triemer, R. E. (1985). A rapid simple technique utilizing calcofluor white M2R for the visualization of dinoflagellate thecal plates. *J. Phycol.* 21, 662–664. doi: 10.1111/j.0022-3646.1985.00662.x
- Gárate-Lizárraga, I., Band-Schmidt, C. J., Verdugo-Díaz, G., Muñetón-Gómez, M., and Félix-Pico, E. F. (2007). “Dinoflagelados (Dinophyceae) del sistema lagunar Magdalena-Almejas,” in *Estudios Ecológicos en Bahía Magdalena*, eds R. Funes-Rodríguez and B. C. S. La Paz (Lund: CICIMAR-IPN), 145–175.
- GBIF.Org (2020). *GBIF Home Page [Online]*. Available: <https://www.gbif.org> (accessed December 05, 2020).
- Glibert, P. M., Burkholder, J. M., and Kana, T. M. (2012). Recent insights about relationships between nutrient availability, forms, and stoichiometry, and the distribution, ecophysiology, and food web effects of pelagic and benthic *Prorocentrum* species. *Harmful Algae* 14, 231–259.
- Gottschling, M., Keupp, H., Plötner, J., Knop, R., Willems, H., and Kirsch, M. (2005). Phylogeny of calcareous dinoflagellates as inferred from ITS and ribosomal sequence data. *Mol. Phylogenet. Evol.* 36, 444–455. doi: 10.1016/j.ympev.2005.03.036
- Gottschling, M., and Plötner, J. (2004). Secondary structure models of the nuclear internal transcribed spacer regions and 5.8 S rRNA in Calciodinelloideae (Peridiniaceae) and other dinoflagellates. *Nucleic Acids Res.* 32, 307–315. doi: 10.1093/nar/gkh168
- Grzebyk, D., Sako, Y., and Berland, B. (1998). Phylogenetic analysis of nine species of *Prorocentrum* (Dinophyceae) inferred from 18S ribosomal DNA sequences, morphological comparisons, and description of *Prorocentrum panamensis*, sp. nov. *J. Phycol.* 34, 1055–1068. doi: 10.1046/j.1529-8817.1998.341055.x
- Herrera-Sepúlveda, A., Medlin, L. K., Murugan, G., Sierra-Beltrán, A. P., Cruz-Villacorta, A. A., and Hernández-Saavedra, N. Y. (2015). Are *Prorocentrum hoffmannianum* and *Prorocentrum belizeanum* (Dinophyceae, Prorocentrales) the same species? An integration of morphological and molecular data. *J. Phycol.* 51, 173–188. doi: 10.1111/jpy.12265
- Hoppenrath, M., Chomérat, N., Horiguchi, T., Schweikert, M., Nagahama, Y., and Murray, S. (2013). Taxonomy and phylogeny of the benthic *Prorocentrum* species (Dinophyceae)—A proposal and review. *Harmful Algae* 27, 1–28. doi: 10.1016/j.hal.2013.03.006
- Hoppenrath, M., Murray, S. A., Chomérat, N., and Horiguchi, T. (2014). *Marine Benthic Dinoflagellates—Unveiling Their Worldwide Biodiversity*. Stuttgart: Schweizerbart'sche Verlagsbuchhandlung.
- Hu, T., Leblanc, P., Burton, I. W., Walter, J. A., Mccarron, P., Melanson, J. E., et al. (2017). Sulfated diesters of okadaic acid and DTX-1: self-protective precursors of diarrhetic shellfish poisoning (DSP) toxins. *Harmful Algae* 63, 85–93. doi: 10.1016/j.hal.2017.01.012
- Hu, W., Xu, J., Sinkkonen, J., and Wu, J. (2010). Polyketides from marine dinoflagellates of the genus *Prorocentrum*, biosynthetic origin and bioactivity of their okadaic acid analogues. *Mini Rev. Med. Chem.* 10, 51–61. doi: 10.2174/138955710791112541
- Huelsensbeck, J. P., Larget, B., and Alfaro, M. E. (2004). Bayesian phylogenetic model selection using reversible jump Markov chain Monte Carlo. *Mol. Biol. Evol.* 21, 1123–1133. doi: 10.1093/molbev/msh123
- Huelsensbeck, J. P., and Rannala, B. (2004). Frequentist properties of Bayesian posterior probabilities of phylogenetic trees under simple and complex substitution models. *Syst. Biol.* 53, 904–913. doi: 10.1080/10635150490522629
- John, U., Litaker, R. W., Montresor, M., Murray, S., Brosnahan, M. L., and Anderson, D. M. (2014). Formal revision of the *Alexandrium tamarense* species complex (Dinophyceae) taxonomy: the introduction of five species with emphasis on molecular-based (rDNA) classification. *Protist* 165, 779–804. doi: 10.1016/j.protis.2014.10.001
- Katoh, K., and Standley, D. M. (2016). A simple method to control over-alignment in the MAFFT multiple sequence alignment program. *Bioinformatics* 32, 1933–1942. doi: 10.1093/bioinformatics/btw108
- Keller, M. D., Selvin, R. C., Claus, W., and Guillard, R. R. (1987). Media for the culture of oceanic ultraphytoplankton. *J. Phycol.* 23, 633–638.
- Koetschan, C., Förster, F., Keller, A., Schleicher, T., Ruderisch, B., Schwarz, R., et al. (2010). The ITS2 Database III—sequences and structures for phylogeny. *Nucleic Acids Res.* 38, D275–D279.
- Krock, B., Tillmann, U., John, U., and Cembella, A. (2008). LC-MS-MS aboard ship: tandem mass spectrometry in the search for phycotoxins and novel toxigenic plankton from the North Sea. *Anal. Bioanal. Chem.* 392, 797–803. doi: 10.1007/s00216-008-2221-7

- Lassus, P., Chomérat, N., Hess, P., and Nézan, E. (2016). *Toxic and Harmful Microalgae of the World Ocean – Micro-algues Toxique et Nuisibles de l’Océan Mondial*. Lausanne: IOC.
- Lim, A. S., Jeong, H. J., Jang, T. Y., Kang, N. S., Lee, S. Y., Du Yoo, Y., et al. (2013). Morphology and molecular characterization of the epiphytic dinoflagellate *Prorocentrum* cf. *rhathymum* in temperate waters off Jeju Island, Korea. *Ocean Sci. J.* 48, 1–17.
- Lim, Z. F., Luo, Z., Lee, L. K., Hii, K. S., Teng, S. T., Chan, L. L., et al. (2019). Taxonomy and toxicity of *Prorocentrum* from Perhentian Islands (Malaysia), with a description of a non-toxic species *Prorocentrum malayense* sp. nov. (Dinophyceae). *Harmful Algae* 83, 95–108. doi: 10.1016/j.hal.2019.01.007
- Loeblich, A. R. III, Sherley, J. L., and Schmidt, R. J. (1979). The correct position of flagellar insertion in *Prorocentrum* and description of *Prorocentrum rhathymum* sp. nov. (Pyrrhophyta). *J. Plankton Res.* 1, 113–120.
- Luo, Z., Zhang, H., Krock, B., Lu, S., Yang, W., and Gu, H. (2017). Morphology, molecular phylogeny and okadaic acid production of epibenthic *Prorocentrum* (Dinophyceae) species from the northern South China Sea. *Algal Res.* 22, 14–30. doi: 10.1016/j.algal.2016.11.020
- Maddison, W. P., and Maddison, D. R. (2019). *Mesquite: A Modular System for Evolutionary Analysis. Version 3.61*.
- Mertens, K. N., Gu, H., Pospelova, V., Chomérat, N., Nézan, E., Gurdebeke, P. R., et al. (2017). First record of resting cysts of the benthic dinoflagellate *Prorocentrum leve* in a natural reservoir in Gujan-Mestras, Gironde, France. *J. Phycol.* 53, 1193–1205. doi: 10.1111/jpy.12582
- Miller, M. A., Pfeiffer, W., and Schwartz, T. (2010). “Creating the CIPRES science gateway for inference of large phylogenetic trees,” in *Proceedings of the 2010 Gateway Computing Environments Workshop (GCE)* (Piscataway, NY: IEEE), 1–8.
- Minh, B. Q., Nguyen, M. A. T., and Von Haeseler, A. (2013). Ultrafast approximation for phylogenetic bootstrap. *Mol. Biol. Evol.* 30, 1188–1195. doi: 10.1093/molbev/mst024
- Moreira-González, A. R., Fernandes, L. F., Uchida, H., Uesugi, A., Suzuki, T., Chomérat, N., et al. (2019). Morphology, growth, toxin production, and toxicity of cultured marine benthic dinoflagellates from Brazil and Cuba. *J. Appl. Phycol.* 31, 3699–3719. doi: 10.1007/s10811-019-01855-0
- Morrison, D. A. (2015). Is sequence alignment an art or a science? *Syst. Bot.* 40, 14–26. doi: 10.1600/036364415x686305
- Nagahama, Y., Murray, S., Tomaru, A., and Fukuyo, Y. (2011). Species boundaries in the toxic dinoflagellate *Prorocentrum lima* (Dinophyceae, Prorocentrales), based on morphological and phylogenetic characters. *J. Phycol.* 47, 178–189.
- Nascimento, S. M., Mendes, M. C. Q., Menezes, M., Rodriguez, F., Alves-De-Souza, C., Branco, S., et al. (2017). Morphology and phylogeny of *Prorocentrum caipirignum* sp. nov. (Dinophyceae), a new tropical toxic benthic dinoflagellate. *Harmful Algae* 70, 73–89. doi: 10.1016/j.hal.2017.11.001
- Nguyen, L.-T., Schmidt, H. A., Von Haeseler, A., and Minh, B. Q. (2014). IQ-TREE: a fast and effective stochastic algorithm for estimating maximum-likelihood phylogenies. *Mol. Biol. Evol.* 32, 268–274. doi: 10.1093/molbev/msu300
- Nielsen, L. T., Krock, B., and Hansen, P. J. (2013). Production and excretion of okadaic acid, pectenotoxin-2 and a novel dinophysistoxin from the DSP-causing marine dinoflagellate *Dinophysis acuta* – Effects of light, food availability and growth phase. *Harmful Algae* 23, 34–45. doi: 10.1016/j.hal.2012.12.004
- Okolodkov, Y. B., Campos-Bautista, G., Gárate-Lizárraga, I., González-González, J. A. G., Hoppenrath, M., and Arenas, V. (2007). Seasonal changes of benthic and epiphytic dinoflagellates in the Veracruz reef zone, Gulf of Mexico. *Aquat. Microb. Ecol.* 47, 223–237. doi: 10.3354/ame047223
- Okolodkov, Y. B., and Gárate-Lizárraga, I. (2006). An annotated checklist of dinoflagellates (Dinophyceae) from the Mexican Pacific. *Acta Bot. Mex.* 1, 1–154. doi: 10.21829/abm74.2006.1008
- Okolodkov, Y. B., Virgilio, F. D. C. M., Castillo, J. A. A., Trujillo, A. C. A., Espinosa-Matias, S., and Silveira, A. H. (2014). Seasonal changes in epiphytic dinoflagellate assemblages near the northern coast of the Yucatan Peninsula, Gulf of Mexico. *Acta Bot. Mex.* 3, 121–151.
- Parsons, M. L., and Preskitt, L. B. (2007). A survey of epiphytic dinoflagellates from the coastal waters of the island of Hawai‘i. *Harmful Algae* 6, 658–669.
- R Core Team (2020). *R: A Language and Environment for Statistical Computing*. Vienna: R Foundation for Statistical Computing.
- Rambaut, A., Drummond, A. J., Xie, D., Baele, G., and Suchard, M. A. (2018). Posterior summarization in Bayesian phylogenetics using Tracer 1.7. *Syst. Biol.* 67:901. doi: 10.1093/sysbio/syy032
- Ronquist, F., Teslenko, M., Van Der Mark, P., Ayres, D. L., Darling, A., Höhna, S., et al. (2012). MrBayes 3.2: efficient Bayesian phylogenetic inference and model choice across a large model space. *Syst. Biol.* 61, 539–542. doi: 10.1093/sysbio/sys029
- RStudio-Team (2020). *RStudio: Integrated Development for R*. Boston, MA: RStudio.
- Seibel, P. N., Müller, T., Dandekar, T., Schultz, J., and Wolf, M. (2006). 4SALE—a tool for synchronous RNA sequence and secondary structure alignment and editing. *BMC Bioinformatics* 7:1–7. doi: 10.1261/rna.232907
- Steidinger, K., and Tangen, K. (1996). “Dinoflagellates,” in *Identifying Marine Diatoms and Dinoflagellates*, ed. C. R. Tomas (California: Academic Press), 387–403.
- Tarazona-Janampa, U. I., Cembella, A. D., Pelayo-Zárate, M. C., Pajares, S., Márquez-Valdelamar, L. M., Okolodkov, Y. B., et al. (2020). Associated bacteria and their effects on growth and toxigenicity of the dinoflagellate *Prorocentrum lima* species complex from epibenthic substrates along Mexican coasts. *Front. Mar. Sci.* 7:569.
- Xie, W., Lewis, P. O., Fan, Y., Kuo, L., and Chen, M.-H. (2011). Improving marginal likelihood estimation for Bayesian phylogenetic model selection. *Syst. Biol.* 60, 150–160. doi: 10.1093/sysbio/syq085
- Yang, Z. (1994). Maximum likelihood phylogenetic estimation from DNA sequences with variable rates over sites: approximate methods. *J. Mol. Evol.* 39, 306–314. doi: 10.1007/bf00160154
- Yasumoto, T., Murata, M., Oshima, Y., Matsumoto, G. K., and Clardy, J. (1984). *Diarrhetic Shellfish Poisoning*. London: ACS Publications, 207–214.
- Zhang, H., Li, Y., Cen, J., Wang, H., Cui, L., Dong, Y., et al. (2015). Morphotypes of *Prorocentrum lima* (Dinophyceae) from Hainan island, South China Sea: morphological and molecular characterization. *Phycologia* 54, 503–516. doi: 10.2216/15-8.1

**Conflict of Interest:** The authors declare that the research was conducted in the absence of any commercial or financial relationships that could be construed as a potential conflict of interest.

**Publisher’s Note:** All claims expressed in this article are solely those of the authors and do not necessarily represent those of their affiliated organizations, or those of the publisher, the editors and the reviewers. Any product that may be evaluated in this article, or claim that may be made by its manufacturer, is not guaranteed or endorsed by the publisher.

Copyright © 2021 Cembella, Durán-Riveroll, Tarazona-Janampa, Okolodkov, García-Sandoval, Krock, Hörstmann and John. This is an open-access article distributed under the terms of the Creative Commons Attribution License (CC BY). The use, distribution or reproduction in other forums is permitted, provided the original author(s) and the copyright owner(s) are credited and that the original publication in this journal is cited, in accordance with accepted academic practice. No use, distribution or reproduction is permitted which does not comply with these terms.